① EPRI-217-1-TR2
② PB-246 254

PB-246 254

FRACTURE MECHANICS AND RESIDUAL FATIGUE LIFE ANALYSIS FOR COMPLEX STRESS FIELDS

P. M. Besuner

Failure Analysis Associates

Prepared for:

Electric Power Research Institute

July 1975

LR-24793

Fracture Mechanics and Residual Fatigue Life Analysis for Complex Stress Fields

Keywords:
Computational Methods
Crack Propagation
Fatigue
Fracture Mechanics
Pressure Vessel
Residual Stress
Stress Gradients
Structural Analysis

EPRI

EPRI 217-1
Technical Report 2
July 1975

: PB 246 254

Prepared by
Failure Analysis Associates
Palo Alto, California 94304

BIBLIOGRAPHIC DATA SHEET	1. Report No. EPRI 217-1 Technical Rpt. #2	2.	3. Recipient's Accession No. PB 246 254
4. Title and Subtitle Fracture Mechanics and Residual Fatigue Life Analysis for Complex Stress Fields			5. Report Date July 1975 6.
7. Author(s) P. M. Besuner			8. Performing Organization Rept. No.
9. Performing Organization Name and Address Failure Analysis Associates Palo Alto, CA 94304			10. Project/Task/Work Unit No. RP 217-1 11. Contract/Grant No.
12. Sponsoring Organization Name and Address Electric Power Research Institute 3412 Hillview Avenue Palo Alto, CA 94304			13. Type of Report & Period Covered Technical Report 14

15. Supplementary Notes CONTINUING RESEARCH....

16. Abstract This report reviews the development and application of an influence function method for calculating stress intensity factors and residual fatigue life for two-and three-dimensional structures with complex stress fields and geometries. Through elastic superposition, the method properly accounts for redistribution of stress as the crack grows through the structure. The analytical methods utilized and the computer programs necessary for computation and application of load independent influence functions are presented. A new exact solution is obtained for the buried elliptical crack, under an arbitrary Mode I stress field, for stress intensity factors at four positions around the crack front. The IF method is then applied to two fracture mechanics problems with complex stress fields and geometries. These problems are of current interest to the electric power generating industry and include (1) the fatique analysis of a crack in a pipe weld under nominal and residual stresses and (2) fatique analysis of a reactor pressure vessel nozzle corner crack under a complex bivariate stress field.

17. Key Words and Document Analysis. 17a. Descriptors

Computational Methods
Crack Propagation
Fatigue
Fracture Mechanics
Pressure Vessel
Residual Stress
Stress Gradients
Structural Analysis

17b. Identifiers/Open-Ended Terms

17c. COSATI Field/Group

18. Availability Statement
RELEASE UNLIMITED

19. Security Class (This Report) UNCLASSIFIED
20. Security Class (This Page) UNCLASSIFIED
21. No. of Pages 88
22. Price

THE INFLUENCE FUNCTION METHOD FOR FRACTURE MECHANICS AND RESIDUAL FATIGUE LIFE ANALYSIS OF CRACKED COMPONENTS UNDER COMPLEX STRESS FIELDS

Research Project 217-1
(FAA-75-4-10)

Technical Report 2

July 1975

Prepared by
P. M. Besuner, Author

Failure Analysis Associates
750 Welch Road
Palo Alto, California 94304

Prepared for

Electric Power Research Institute
3412 Hillview Avenue
Palo Alto, California 94304

F. Gelhaus, Project Manager

NOTICE

This report was prepared by Failure Analysis Associates as an account of work sponsored by the Electric Power Research Institute, Inc. (EPRI). Neither EPRI, members of EPRI, Failure Analysis Associates, or any person acting on behalf of either: (a) makes any warranty or representation, express or implied, with respect to the accuracy, completeness, or usefulness of the information contained in this report, or that the use of any information, apparatus, method, or process disclosed in this report may not infringe privately owned rights; or (b) assumes any liabilities with respect to the use of, or for damages resulting from the use of, any information, apparatus, method, or process disclosed in this report.

ABSTRACT

This report reviews the development and application of an influence function method for calculating stress intensity factors and residual fatigue life for two-and three-dimensional structures with complex stress fields and geometries. Through elastic superposition, the method properly accounts for redistribution of stress as the crack grows through the structure. The analytical methods utilized and the computer programs necessary for computation and application of load independent influence functions are presented. A new exact solution is obtained for the buried elliptical crack, under an arbitrary Mode I stress field, for stress intensity factors at four positions around the crack front. The IF method is then applied to two fracture mechanics problems with complex stress fields and geometries. These problems are of current interest to the electric power generating industry and include (1) the fatigue analysis of a crack in a pipe weld under nominal and residual stresses and (2) fatigue analysis of a reactor pressure vessel nozzle corner crack under a complex bivariate stress field.

TABLE OF CONTENTS

the crack explicitly in the stress analysis for each crack size. Furthermore, the influence function, h, which depends only on geometry, can be accurately obtained from relatively simple loading conditions and applied to complex stress fields.

The following sections provide more detailed description of the IF method. Section 2 presents the basic methodology and Section 3 and Appendices A and B discuss methods for accurate and efficient computation of h and K for two- and three-dimensional problems. Section 3 also reviews available h solutions and computer programs including a new exact three-dimensional solution, derived in Appendix C, for the K values of the four symmetry positions around the periphery of a buried elliptical crack under arbitrary Mode I stress fields. Section 4 describes the use of the IF method to predict residual fatigue lives for two- and three-dimensional crack problems.

Finally, the IF method is applied to two engineering fracture mechanics problems of interest to the electric power generating industry. Applicability to two-dimensional problems is demonstrated in Section 5 with a fatigue analysis example that accounts for both the nominal stresses and the non-uniform residual stresses acting on a through-crack oriented perpendicular to a circumferential weld in a large pipe, and in a finite width specimen.

A most important feature of the IF method is its applicability to three-dimension problems. Here, the IF method accounts for the complications of complex stress fields, crack shape, crack shape change during growth and K variation along the crack front. Applicability to three-dimensional problems with large stress gradients is demonstrated in Section 6 through a fatigue analysis of a corner crack in the nozzle of a thick walled pressure vessel.

2.0 GENERAL DESCRIPTION OF THE INFLUENCE FUNCTION METHOD

The IF method has been previously described in (1-9)* for two-dimensional elastic crack problems and in (9-11) for three-dimensional problems. This section reviews only the major concepts of the IF method. Fig. 1 illustrates the elastic superposition principle which is the basis of the IF method. The superposition reduces the K solution of an arbitrary and, perhaps, difficult crack problem to the solution of (1) the problem without the crack (i.e. uncracked problem), and (2) a crack problem in which only the crack face is pressurized so as to cancel the uncracked stresses ($\sigma(x)$ in Fig. 1) that would exist across the crack locus in the absence of the crack. Influence functions are used to solve this second, pressurized crack problem. An influence function h is simply the K value arising from a unit point load at some position, usually on the crack face. Thus h is independent of loading, as proven rigorously in (9), and depends only on the crack face position and structural geometry.

To solve the pressurized crack problem, and, hence, the difficult original problem, consider first the differential load $\sigma(x)\,dx$ (assuming constant thickness) which causes a differential increment of K given by

$$dK(x) = h\,(x, \text{geometry})\ \sigma(x)\,dx \tag{2.1}$$

so that the stress intensity factor is given by

$$K = \int_{L_a} dK(x) = \int_{L_a} h(x,\text{geo.})\ \sigma(x)dx \tag{2.2}$$

where L_a is the straight crack face boundary parallel to the x axis.

*Underlined numbers enclosed in parentheses refer to references listed at the end of the report.

To illustrate the utility of (2.2), consider the center-cracked plate under symmetric loading shown in Fig. 2. For the case of uniform stress on an infinite plate ($a/b \to 0$), the stress intensity factor is given by

$$K = \sigma_o \sqrt{\pi a} \tag{2.3}$$

where a is the half crack length and σ_o is the applied uniform stress. It has been shown by Paris (3) that, for any symmetric stress field, $\sigma(x) = \sigma(-x)$, the influence function for the infinite plate is given by

$$h = \frac{2}{\sqrt{\pi}} \left(\frac{a}{a^2 - x^2} \right)^{1/2}, \quad 0 \leq x \leq a \text{ defines } L_a \tag{2.4}$$

Equations (2.2) and (2.4) reduce to Equation (2.3) for the case of constant $\sigma(x) = \sigma_o$.

Thus, we see by example that the IF method can correctly quantify the crack-induced redistribution of the uncracked elastic stress field. The utility of the influence function method for handling complex stress fields becomes clear once it is realized that if h is obtained for a particular cracked geometry with several variable dimensional parameters, K computation is reduced to:

A. Determination and specification of the uncracked stress field, and

B. Numerical integration of Equation (2.2), for the appropriate crack geometry.

The next section documents the references, procedures, and methods required for accurate computation of h for a variety of simple geometries sufficient to solve a majority of structural problems.

3.0 BASIC EQUATIONS AND AVAILABLE SOLUTIONS OF THE INFLUENCE FUNCTION METHOD

The most direct method to solve for h is to obtain a solution for K due to a point load at any crack face location. Table I outlines the published sources of h solutions and the computer algorithms, developed and modified by the author at Failure Analysis Associates, that use h to compute K. The table shows that a formidable selection of h solutions already exists to handle cracks in complex stress gradients. If a point load solution is not directly available nor easily derivable, the formulations below provide practical methods to determine h.

3.1 Basic Equations to Determine Influence Functions and Stress Intensity Factors

The root-mean-square (rms) stress intensity factor, $\bar{K}$, has been defined in (10) as an integrated average of K(s) (the specific value of the stress intensity factor K along the crack front at point s) over the new surface area created by selected virtual displacement of the crack front. In the case of two-dimensional elasticity problems, K(s) is constant, and $\bar{K}$ and K(s) are identical. Consequently, $\bar{K}$ and K are used interchangeably for two-dimensional problems throughout the remainder of this report. K and $\bar{K}$ are not exactly equivalent for most three-dimensional problems, since K(s) is not, in general, constant. However, K and $\bar{K}$ are similar enough for most three-dimensional crack problems to lead to nearly identical static strength or fatigue life estimates (10).

Consider now a two- or three-dimensional crack problem for which there are n degrees of freedom (DOF), where a DOF is defined as that scalar dimension or variable which is free to increase (e.g. propagate in fatigue) and do work independently of all other dimensions or variables. Then $\bar{K}$ due to a small perturbation of the j-th DOF (Fig. 3) may be expressed as (10, 11)

$$\bar{K}_j = \int_A h_j\,(x_i,\ \text{geometry})\ \sigma\,(x_i)\ dA;\quad j = 1,\ n,\ i = 1,\ n_i \qquad (3.1)\dagger$$

where A represents the crack area, x_i are the appropriate coordinate directions, (n_i = 2 or 3) σ is the uncracked stress field, and h_j is the influence function for the j-th of n DOF's and is given by (10, 11) as

$$h_j\,(x_i,\ \text{geometry}) = \frac{H}{\bar{K}^*_j}\ \frac{\partial w^*}{\partial A_j} \qquad (3.2)$$

where

$$\frac{\partial}{\partial A_j} = \frac{\partial a_j}{\partial A}\ \frac{\partial}{\partial a_j} \qquad (3.3)$$

In (3.1) and (3.2),

$\bar{K}_j$ = rms stress intensity factor due to perturbation of the j-th DOF only,

w = crack opening displacement for the top half of the crack only, and

H = appropriate modulus

$$H = \frac{E}{1-\nu^2},\ \text{for isotropic plane strain}$$
$$H = E,\ \text{for isotropic plane stress} \qquad (3.4)$$

and, for certain classes of orthotropic material problems, H is given on page D-3 of (6). The superscript (*) indicates $\bar{K}_j$ and w values determined for the given geometry for some arbitrary reference state of loading.

$\bar{K}^*_j$, may be rewritten in terms of the strain energy, U*, as

$$\bar{K}^*_j = \left(H\ \frac{\partial U^*}{\partial A_j}\right)^{1/2} \qquad (3.5)$$

†In this report, repeated subscript indices do not imply summation.

Combining Equations (3.2, 3.3, 3.5) then gives the final form of the influence function as

$$h_j = \left(\frac{1}{H} \frac{\partial A}{\partial a_j} \frac{\partial U^*}{\partial a_j} \right)^{-1/2} \frac{\partial w^*}{\partial a_j} \qquad (3.6)$$

It is seen from equation (3.6) that one need only determine the strain energy and crack opening displacement for any single, simple reference stress field applied to the given crack and structural geometry to determine h_j. For some simple problems these quantities are known by exact closed form expressions. They can also be measured experimentally (12) or, more commonly, can be determined using numerical stress analysis techniques. The analytical and numerical methods are described in some detail in Appendices A, B, and C for three cases of increasing complexity: a two-dimensional crack with one DOF for crack propagation, a three-dimensional crack with two DOF, (both size and shape may change), and a three-dimensional crack with four DOF (size, shape, and centroid of the crack may change).

3.2 Some Exact and Approximate Influence Function Solutions

Table I lists source information for influence functions for many geometries of interest. For convenience, all influence functions utilized in Sections 5 and 6 are given below.

3.2.1 Center-Cracked Strip

Fig. 2 shows a symetrically loaded center-cracked strip of width 2b.

The influence functions for all three loading modes for this two-dimensional problem are given in (6) as

$$h_{III} = \left[\frac{2ca\pi}{b} \left[1 - \left(\frac{\cos \frac{\pi a}{2b}}{\cos \frac{\pi x}{2b}} \right)^2 \right] \right]^{\frac{1}{2}} \text{(exact solution)} \qquad (3.7)$$

$$h_I = h_{II} = \left\{ 1+0.2967\sqrt{1-(x/a)^2} \quad (1-\cos \frac{\pi a}{2b}) \right\} h_{III} \quad (\pm 1\% \text{ error}) \qquad (3.8)$$

In the limit of infinite width ($\frac{a}{2b} \longrightarrow 0$), the functions for all three modes reduce to (2.4). Equations (3.7, 3.8) have been programmed and the subroutine (IF2-1) is listed as part of Appendix D and applied in Section 4. Both IF2-1 and a published solution are used in Table II to compute K for a finite width plate under uniform stress. The excellent agreement between solutions confirms the accuracy of the two-dimensional IF computer method for this geometry.

3.2.2 The Two-Degree-of-Freedom Buried Elliptical Crack

Reference (10) presents the exact h and K_I solution to this problem (Fig. 6) for the case of arbitrary Mode I loading, σ_{zz} (x, y), across the elliptical crack with major and minor axes a_y and a_x in the x-y plane. The solution is derived by substitution of the appropriate displacement and strain energy expressions in Appendix B into (3.6) and (3.1) to obtain

$$\bar{K}_x = \frac{\iint_A \left(\frac{1}{a_x} - \frac{\partial E(k)}{E(k)\partial a_x} + \frac{x^2}{a_x^3 \alpha} \right) \alpha^{1/2} \sigma_{zz}(x,y)\, dA}{\pi a_y \left[\frac{E(k)}{3} \left(\frac{2}{a_x} - \frac{\partial E(k)}{E(k)\partial a_x} \right) \right]^{1/2}}$$

$$\bar{K}_y = \frac{\iint_A \left(- \frac{\partial E(k)}{E(k)\, a_y} + \frac{y^2}{a_y^3 \alpha} \right) \alpha^{1/2} \sigma_{zz}(x,y)\, dA}{\pi \left[\frac{a_x a_y E(k)}{3} \left(\frac{1}{a_y} - \frac{\partial E(k)}{E(K)\partial a_y} \right) \right]^{1/2}} \qquad (3.9)$$

In (3.9), $E(k)$ is the complete elliptic integral of the second kind with $k^2 = 1-(a_x/a_y)^2$ and $\alpha = 1 - (x/a_x)^2 - (y/a_y)^2$.

The area integrals of the above expressions are evaluated numerically using a rectangular partitioning scheme with a refined grid near the crack front, $\alpha \longrightarrow 0$, to account for the $\alpha^{-1/2}$ singularity. Trial-and-error has shown that for all 30-40 test cases investigated, with exact solutions for $\bar{K}_i$, 300 rectangular partitions are sufficient to obtain $\bar{K}_x$ and $\bar{K}_y$ with less than 2.5% error and in less than three seconds central processing unit (CPU) time on the IBM 360-67 computer. Table III compares the three-dimensional IF computer code (IF3-3) calculations with the exact solution for a circular crack under two complex stress fields.

3.2.3 The Two-Degree-of-Freedom Quarter Ellipse Corner Crack in a Quarter Space

Reference (11) applies a three-dimensional boundary-integral equation computer program (17) with Equations (3.1, 3.6) to obtain an accurate numerical solution to this problem pictured in Figs. 5 and 7. Also, a fairly accurate approximate solution can be obtained using a two-dimensional analog from (20). Appendix B presents the approximate solution method which, typically, leads to $\bar{K}$ computations within 5% of those resulting from the rigorous, full three-dimensional analyses used in (11).

3.2.4 The Two-Degree-of-Freedom Half-Ellipse Surface Crack in a Half Space

Appendix B uses the two-dimensional analog mentioned above to obtain approximate solutions to this problem, illustrated in Fig. 7.

3.2.5 Three-Dimensional Problems with Finite Width and Other Effects That Must be Evaluated Numerically

As discussed previously in this section, both analytical (11, 17) and experimental (12) three-dimensional solution capabilities exist to obtain crack face displacements to compute the h_j and K_j with Equations (3.6, 3.1).

3.2.6 The Four-Degree-of-Freedom Buried Elliptical Crack

Appendix C presents a new exact solution for h_j and $\bar{K}_j$, $j = 1, 4$ for the four DOF buried elliptical crack shown in Fig. 8. This four DOF model allows independent growth of the major and minor elliptical axes and also translation of the crack centroid. In other words, opposite ends of both the major and minor axes can grow at different rates. Four DOF are necessary to analyze crack growth under stress fields $\sigma(x',y')$ that are not symmetric with respect to the elliptical axes.

4.0 RESIDUAL FATIGUE LIFETIME PREDICTION METHODOLOGY

The use of two- and three-dimensional fracture mechanics analysis to predict the residual lifetime of sharply notched or cracked structures has been described in many previous papers (e.g. 2, 10, 11, 18, 19). Previous literature has defined the three basic inputs to fracture mechanics lifetime prediction as: (1) the experimental evaluation of the material's crack propagation law under the appropriate thermal-mechanical loading cycle, (2) methods for the analytical calculation of crack tip strain intensity factors, and (3) methods (e.g. nondestructive inspection) for accurately defining initial flaws and early detection of crack initiation. A procedure that utilizes the IF method in conjunction with these three elements is presented in general terms below and is adapted for specific applications in the next two sections.

4.1 Two- or Three-Dimensional Crack Propagation Analysis Procedure

The basis of reported life analyses is the notion of a finite number, n, of characteristic dimensions a_i; i = 1, n, to describe crack geometry. Crack propagation is then described by keeping track of the a_i which are called degrees of freedom or DOF. The continuous stress intensity factor function K(s) is similarly approximated with a set of discrete stress intensity factors K_i; i = 1, n, each associated with an a_i. The applied general empirical model of three-dimensional propagation is then expressed by n equations.

$$\frac{da_i}{dN} = F \quad (K_i, \text{Material, Environment, History}) \qquad (4.1)$$

where

N = residual lifetime;

K_i = stress intensity factor associated with a_i; and

F = empirically determined function.

Each equation in (4.1) states that the instantaneous cyclic growth rate da_i/dN of freedom a_i is given by the empirically determined function F. Further, (4.1) implies that all load and geometry information relevant to da_i/dN is contained in one and only one stress intensity factor K_i. The function F is independent of load and geometry and may be obtained in the traditional way from simple planar laboratory specimens. The stress intensity factors K_i each contain an alternating component ΔK_i and mean value K_{mean_i} associated with the alternating and mean components of the stress cycle, $\Delta\sigma$ and σ_{mean}.

Residual life prediction is accomplished by formulation and solution of (4.1) A four-step method is employed for life prediction. The steps are:

(1) Obtain F from simple specimens. F is often expressed in the form of piecewise power functions of ΔK (e.g. $da/dN = C\Delta K^n$) for given K_{mean}, material, environment and history combinations.

(2) Determine the uncracked structural detail geometry, loads, and, to the extent required by step 3, stress.

(3) Model the propagating crack. This task includes selection of a model with an adequate number of DOF, specification of the initial and final crack configuration a_{Ii} and a_{Fi} and definition of K_i. Further, an FE method-based algorithm is derived to compute all of the K_i as functions of stress and geometry, especially the changing crack geometry a_i.

(4) Substitute K_i in (4.1) and solve for the life N.

The above procedure has been successfully applied to predict fatigue lives in many instances where accurate uncracked stress and material crack growth rate data were available. Published examples of two-dimensional analyses

in (21) and three-dimensional analyses in (11) exemplify the good agreement obtained between calculated and observed fatigue crack growth. Additional examples of fatigue growth calculations for a weld crack and a vessel or pipe nozzle detail are described in the following sections.

5.0 FATIGUE ANALYSIS OF A WELD CRACK

A weld seam under longitudinal (y-direction) load symmetric about the y-axis, with a transverse through-thickness crack of length 2a is illustrated in Fig.9. This section describes the analysis of fatigue growth of the crack for two plate widths. The first width, 2b=10", models a laboratory specimen while the second width, $2b \to \infty$, models the case of a pipe with radius and length substantially larger than 2a. The longitudinal stresses include uniform alternating and mean components, $\Delta\sigma$ and σ_m, respectively, and a complex residual stress field, $\sigma_{res}(x)$, as illustrated in Fig. 9, for the case of the ten-inch specimen. The residual stress function is slightly different for the case of a large pipe because of the additional elastic constraint; both residual stress distributions were estimated from measurements in (22).

Since the subject problem assumes only one DOF, a, (4.1) reduces to only one equation for application of the four-part life prediction procedure given in Section 4. Equation(4.1) must account for the effect of R-ratio, $R=K_{min}/K_{max}$, on da/dN. For simplicity, a crack growth relation suggested by Forman (23) for positive values of R has been applied below for all values of R, and, as is shown in (24), the relation over-predicts da/dN for negative R. The applied crack growtn relationship is based on the weld region material data in (25) and is given by

$$\frac{da}{dN} = 1.4 \times 10^{-7} \Delta K^{2.74} \left\{ K_{1c}(1-R) - \Delta K \right\}^{-1}, \quad K_{max} > 0 \qquad (5.1)$$

$$\frac{da}{dN} = 0, \quad K_{max} < 0$$

where the force, length and time units in (5.1) are kilopounds, inches, and constant-amplitude fatigue cycles, and $K_{max} = \Delta K/(1-R)$. The initial crack length is assumed to be $2a_i = 0.25"$ and the final crack length, $2a_f$, is defined by the fracture toughness

$$K_{max}(a_f) = K_{Ic} = 150 \text{ ksi}(\text{in})^{1/2} \tag{5.2}$$

The above information and Fig. 9 comprise the first two parts of the life calculation procedure and the crack problem model of the third step. A computer program (IF2-1), with complete listing included in Appendix A, has been written to accomplish the remainder of the procedure; namely, the computation of K components using Equations (3.1,3.7,3.8), and the numerical integration of (5.1) to obtain the relationship between crack length and number of fatigue cycles (a vs. N).

Three load cases were analyzed for each of the two geometries as summarized in Table IV. Appendix A lists the tabular computer output for all six cases, and Figs. 10 and 11 present the corresponding a vs. N curves. Figures 10 and 11 both indicate that, for the case of zero minimum stress, $\sigma_m = \sigma/2 = 12.5$ ksi, the residual stress significantly increases the crack growth rate in the early stage and substantially reduces overall fatigue life. The two figures also show that, even for the the case of applied cyclic compression, corresponding to $\sigma_m = -17.5$ ksi, the positive residual stresses permit some initial growth of the crack followed by subsequent arrest at $K_{max} = 0$ in Eqn. (5.1).

6.0 FATIGUE ANALYSIS OF A PRESSURE VESSEL NOZZLE CORNER CRACK

Figure 12 shows the normalized stress $\sigma(x,y)$ contours computed in (26) for a 1000 psi internal pressure at the pipe-nozzle junction representing an HSST program, intermediate test vessel. Figure 13 shows a hypothetical corner crack of initial dimensions $a_x = a_y = 0.5$ in. at the peak stress location and also gives an equation which, when divided by the factor 4.662, fits the stress contours of Fig. 12 with 0.165 ksi average error. The above factor represents the ratio between the actual and normalized peak stresses estimated in (26) for the heat-up and cooldown vessel operation transient. For simplicity, and due to the lack of a full thermal stress distribution, the stress contours in Fig. 12 are assumed to apply for all loading components (e.g. thermal as well as the pressure loading). However, as demonstrated in Section 5, the IF method is capable of analyzing more complex cases with combined stress distributions and non-proportional loading. The equation in Figure 13 was obtained by multi-parameter least square fit.

Table V lists the vessel-nozzle junction, peak stress levels and the frequencies associated with eleven types of plant operating transients. The Table uses the conservative ASME Code (28) crack growth relation to sum the individual da/dN contributions of all transients and obtain the final crack growth relation

$$\frac{da_i}{dN} = 1.4 \times 10^{-7} \Delta K_i^{3.726}, \quad i=x,y, \tag{6.1}$$

where the force, length, time units of (6.1) are kilopounds, inches, and 40-year increments of plant operation.

The equations to compute $\Delta\bar{K}_i$ are derived from the approximate corner crack (Fig. 7) solution in Appendix B and are given by

$$\bar{K}_x = \frac{\iint_A \left(\frac{1}{a_x} - \frac{\partial E(k)}{E(k)\partial a_x} + \frac{x^2}{a_x^3 \alpha} \right) \alpha^{1/2} (f_s(x_s)+f_s(y_s)-1)\sigma_{zz}(x,y)\, dA}{\pi a_y \left[\frac{E(k)}{3} \left(\frac{2}{a_x} - \frac{\partial E(k)}{E(k)\partial a_x} \right) \right]^{1/2}} \quad (6.2)$$

$$\bar{K}_y = \frac{\iint_A \left(-\frac{\partial E(k)}{E(k)\partial a_y} + \frac{y^2}{a_y^3 \alpha} \right) \alpha^{1/2} (f_s(x_s)+f_s(y_s)-1)\sigma_{zz}(x,y)\, dA}{\pi \left[\frac{a_x a_y E(k)}{3} \left(\frac{1}{a_y} - \frac{\partial E(k)}{E(k)\partial a_y} \right) \right]^{1/2}} \quad (6.3)$$

where f_s is defined in Appendix B.

Equations (6.2) and (6.3) have been incorporated in computer program IF3-3 which also substitutes the $\bar{K}_i$, i = x,y values in (6.1) to compute da_i/dN. The computer program then obtains a_x and a_y as a function of N by solving the two simultaneous differential equations in (6.1) with a modified Hamming's predictor-corrector numerical technique.

Figure 13 gives the results of the three-dimensional fatigue analysis. As seen, the nozzle is estimated to endure 20 to 25 times the expected (28) number of load transients in the 40 year plant operation. The infinite solid model used herein is expected to break down approximately at the "20 N" crack front contour in Fig. 13. As a temporary measure, FAA plans to incorporate appropriate forms of the ASME Code (28) approximate finite width correction factors, such as the subprograms listed in (27), in all its three-dimensional computer programs. A long range goal is to apply a three-dimensional BIE program (17) to compute h rigorously for 3-D finite width geometries with the methods detailed in Section 3.

7.0 CONCLUSIONS

1. The influence function (IF) method is an efficient, general procedure for elastic fracture mechanics analysis of structures with cracks in regions of complex stress.

2. Once influence functions are obtained, the IF method requires only the stresses in the uncracked structural detail and thereby eliminates the need for full two or three-dimensional stress analysis for each considered loading, crack size, shape, and location, and increment of fatigue crack growth.

3. Since influence functions depend only upon geometry, they may be computed from the crack opening displacements for any convenient simple loading that can be accurately solved by analytical, experimental, or numerical techniques. This eliminates the numerical errors caused by inclusion of actual, complex structural loading into computer stress analysis of cracks.

4. The IF method accounts for such three-dimensional complications as complex crack shape, crack shape change during fatigue growth, and variation of the stress intensity factor along the crack front.

5 The extension of the IF method to more complex geometric models is direct, requiring only specification of a model with appropriate number of variable dimensions together with a minimum number of two- or three-dimensional stress analyses to compute the IF. Thus, the majority of crack problems are brought within the scope of an efficient elastic fracture mechanics procedure.

6. The significant effect of residual stress upon fatigue growth of a weld crack has been demonstrated with the IF method.

7. The fatigue growth of an elliptical corner crack in a geometry representative of a reactor pressure vessel nozzle has been analyzed, demonstrating the ease of use of the IF method for a three-dimensional problem with complex stress distribution.

APPENDIX A

Computation of Influence Functions and Stress Intensity Factors for Two-Dimensional Problems

A.1 Calculation of Two-Dimensional Influence Functions, h

Consider a two-dimensional crack, oriented in the x-direction, for which the one degree of freedom is the crack length, a. Then the area increment dA in Equation (3.1) becomes t(x) dx and (3.1) becomes

$$K = \int_X h(x, a, \text{geometry})\ \sigma(x)\ t(x)\ dx \qquad (A.1)$$

Since the area of the crack (assuming unit thickness, t = 1) is simply a, the general equation to compute h (3.6) then becomes

$$h = \left(\frac{1}{H} \frac{\partial U^*}{\partial a} \right)^{-1/2} \frac{\partial w^*}{\partial a} \qquad (A.2)$$

The influence function given by Equation (A.2) may be determined using w* from known, closed-form solutions or calculated from any appropriate numerical stress analysis method, such as finite elements (FE) or boundary-integral equations (BIE), as in (11, 12).

To illustrate the use of analytical displacement solutions to determine h, consider again the simple infinite plate case of the plane stress problem shown in Fig. 2 for which

$$\frac{\partial U^*}{\partial a} = G^* = \frac{K^{*2}}{E} = \frac{\sigma_o^2\, a}{E} , \qquad (A.3)$$

and the crack face displacements are known to be (9)

$$w^* = \frac{2\sigma_o}{E} (a^2 - x^2)^{\frac{1}{2}} \tag{A.4}$$

Therefore

$$\frac{\partial w^*}{\partial a} = \frac{2\sigma_o a}{E(a^2-x^2)^{\frac{1}{2}}} \tag{A.5}$$

and, from (A.2) we compute

$$h = \left(\frac{1}{E} \frac{\sigma_o^2 \pi a}{E}\right)^{-\frac{1}{2}} \frac{2\sigma_o a}{E(a^2-x^2)^{\frac{1}{2}}} = \frac{2}{\sqrt{\pi}} \left(\frac{a}{a^2-x^2}\right)^{\frac{1}{2}} \tag{A.6}$$

which agrees with (2.4).

Numerical stress analysis to determine h, for each crack geometry of interest, can be performed in one of two ways: (1) using two separate stress analyses of slightly different crack size to determine h from incremental differences, or (2) using one stress analysis to determine strain energy and crack opening displacements as mathematical functions of the different DOF, for substitution into Equation (A.2) to determine h. Both methods are illustrated below.

The method of using incremental differences between two stress analyses to obtain h can be illustrated by the problem of a through-the-thickness edge crack in a finite width strip (Fig. 4a). This problem has been solved using a boundary-integral equation program in (13). Special care was taken in modeling the crack, perturbing the crack tip, and choosing the arbitrary reference loading. Experience has shown that the optimum accuracy and efficiency results from a breakup of the crack into equal size segments over about 80% of the total crack length and successively smaller segments near the crack tip,

with approximately a mirror image of this breakup for some distance beyond the crack tip. Perturbation of the crack tip is best accomplished by moving not only the one node at the crack tip, but a series of nodes very near the crack tip (see Fig. 4b). Finally, the most accurate results are obtained when the crack surface is uniformly pressurized. Having solved these two nearly identical stress analyses, the work done by the applied loads (strain energy) for each crack configuration is calculated. Then the incremental changes in strain energy, ΔU, and crack opening displacement, Δw, between the two analyses are computed and these results are used in the incremental form of Equation (A.2) to calculate h,

$$h = \left(\frac{1}{H} \frac{\Delta U}{\Delta a} \right)^{-\frac{1}{2}} \frac{\Delta w}{\Delta a} \qquad (A.7)$$

The second numerical method to determine h requires only one stress analysis for each crack length of interest. Then, U^* and w^* are determined as mathematical functions of crack length (using, for instance, a least-square fit) for substitution into Equation (A.2).

The two-dimensional influence functions can also be obtained using finite element techniques, although such techniques in general require longer modeling times, data preparation times, and computer run times than does the boundary-integral equation method [13]. However, for the specific choice of a uniformly pressurized crack face loading, the finite element-computed influence function results agree with boundary-integral equation results for a large class of problems (no published reference available).

A.2 Calculation of Two-Dimensional K

The best way to use the influence function results, as determined above, to compute K is to ratio those results to numerical results for some simple reference problem geometry. This eliminates most systematic errors which might

be inherent in the stress analysis and avoids the curve fitting of singular h functions. The use of ratios also permits more accurate programming of the stress intensity expressions (for purposes of life calculations, such as in computer programs listed in Table I) provided the solution to the simple reference geometry is known in closed form. Using this method, a new function f may be defined as

$$f = \frac{h}{h'} \tag{A.8}$$

where h' represents the influence function for the reference geometry. Similarly, two new functions g_1 and g_2 may be defined as

$$g_1 = \frac{U}{U'} \qquad g_2 = \frac{w}{w'} \tag{A.9}$$

where the superscript (') again refers to the reference geometry, and the superscript (*) has been dropped for convenience. Combining (A.1) and (A.8) gives

$$K = \int_x f(x, a, \text{geometry})\, h'\, \sigma(x)\, dx \tag{A.10}$$

and combining (A.2), (A.8) and (A.9) gives

$$f = \left(g_1 + U' \left(\frac{\partial U'}{\partial a}\right)^{-1} \frac{\partial g_1}{\partial a} \right)^{-\frac{1}{2}} \left(g_2 + w' \left(\frac{\partial w'}{\partial a}\right)^{-1} \frac{\partial g_2}{\partial a} \right) \tag{A.11}$$

Thus it is seen from Equations (A.10) and (A.11) that the best choice of a reference problem is one for which h' (or U' and w'; from which h' could be determined using Equation (A.2)), is known exactly.

The most convenient two-dimensional reference problem for which a closed form solution is known is a through-the-thickness center crack in an infinite body for which h has already been given in (A.5).

Therefore, f may be determined by combining the results of stress analyses of the actual problem and the reference problem as in Equation (A.8). This f may then be used, with Equation (A.10) to determine K. Thus

$$K = \frac{2}{\sqrt{\pi}} \int_x \left(\frac{a}{a^2-x^2}\right)^{1/2} f\ \sigma(x)\ dx \qquad (A.12)$$

It is best to perform a number of stress analyses in order to determine f, g_1, and g_2 values in terms of the necessary geometric parameters, and then to employ a curve fitting procedure to define expressions for f, g_1 and g_2 which may be used in (A.8 - A.11).

APPENDIX B

Computation of Influence Functions and Stress Intensity Factors for Three-Dimensional Problems

Analytical calculation of h, $\bar{K}$, and K(s) is restricted to a very small class of three-dimensional problems, as indicated by Table I, because of the scarcity of three-dimensional displacement solutions. However, Appendix C and (10) do obtain exact solutions for the elliptical crack problem. Other three-dimensional problems will be solved numerically and/or with approximations derived from analogous two-dimensional solutions.

B.1 Numerical Methods for Three-Dimensional Analysis

The numerical methods described in Appendix A for two-dimensional problems may be extended to three-dimensional problems. Consider a three-dimensional elliptical crack, oriented in the x-y plane, for which the two DOF are the two semi-axes of the ellipse, a_x and a_y. Then dA is dxdy and Equation (3.1) becomes

$$\bar{K}_x = \int\int h_x\,(x, y, a_x, a_y, \text{geometry})\ \sigma(x,y)\ dxdy$$
$$\bar{K}_y = \int\int h_y\,(x, y, a_x, a_y, \text{geometry})\ \sigma(x,y)\ dxdy \qquad (B.1)$$

Since the area of the crack is $\pi a_x a_y$, the influence coefficients h_x and h_y are given by Equation (3.6) as

$$h_x = \left(\frac{\pi a_y}{H} \quad \frac{\partial U^*}{\partial a_x} \right)^{-\frac{1}{2}} \quad \frac{\partial w^*}{\partial a_x}$$

$$h_y = \left(\frac{\pi a_x}{H} \quad \frac{\partial U^*}{\partial a_y} \right)^{-\frac{1}{2}} \quad \frac{\partial w^*}{\partial a_y} \tag{B.2}$$

To illustrate numerical methods to evaluate (B.2), consider the problem of an elliptical corner crack in an infinite body (Fig. 5a). The most efficient current stress analysis technique for three-dimensional crack problems is the boundary-integral equation method (11). Modeling of this problem is illustrated in Fig. 5b and discussed extensively in (11). If two analyses are performed to calculate h, with the incremental difference techniques, care must be taken to perturb only one degree of freedom (one axis) at a time. Equations (A.10) and (A.11) may also be extended to three dimensions so that

$$\bar{K}_x = \int \int f_x\,(x, y, a_x, a_y, \text{geometry})\; h'_x\; \sigma(x,y)\; dxdy$$

$$\bar{K}_y = \int \int f_y\,(x, y, a_x, a_y, \text{geometry})\; h'_y\; \sigma(x,y)\; dxdy \tag{B.3}$$

and

$$f_x = \left(g_1 + U' \left(\frac{\partial U'}{\partial a_x}\right)^{-1} \frac{\partial g_1}{\partial a_x} \right)^{-\frac{1}{2}} \left(g_2 + w' \left(\frac{\partial w'}{\partial a_x}\right)^{-1} \frac{\partial g_2}{\partial a_x} \right)$$

$$f_y = \left(g_1 + U' \left(\frac{\partial U'}{\partial a_y}\right)^{-1} \frac{\partial g_1}{\partial a_y} \right)^{-\frac{1}{2}} \left(g_2 + w' \left(\frac{\partial w'}{\partial a_y}\right)^{-1} \frac{\partial g_2}{\partial a_y} \right) \tag{B.4}$$

The only three-dimensional problem with an exact crack opening displacement solution is the buried elliptical flaw, under uniform pressure, σ_o, for which the strain energy is (14)

$$U' = \frac{4\pi\sigma_o^2 a_x^2 a_y}{3HE(k)} \quad , \tag{B.5}$$

where E(k) is the complete elliptic integral of the second kind with $k^2 = 1-(a_x/a_y)^2$. The crack opening displacement is given by (15) as

$$w = \frac{2\sigma_o a_x}{HE(k)} \alpha^{\frac{1}{2}} \quad , \tag{B.6}$$

where $\alpha=1-(x/a_x)^2 - (y/a_y)^2$. Using Equations (B.5) and (B.6), Equation B.4) then becomes

$$f_x = \left\{ g_1 + \frac{\partial g_1}{\partial a_x} \left[\frac{2}{a_x} - \frac{1}{E(k)} \frac{\partial E(k)}{\partial a_x} \right]^{-1} \right\}^{-\frac{1}{2}} \left\{ g_2 + \frac{\partial g_2}{\partial a_x} \left[\frac{1}{a_x} - \frac{1}{E(k)} \frac{\partial E(k)}{\partial a_x} + \frac{x^2}{a_x^3 \alpha} \right]^{-1} \right\}$$

$$f_y = \left\{ g_1 + \frac{\partial g_1}{\partial a_y} \left[\frac{1}{a_y} - \frac{1}{E(k)} \frac{\partial E(k)}{\partial a_y} \right]^{-1} \right\}^{-\frac{1}{2}} \left\{ g_2 + \frac{\partial g_2}{\partial a_y} \left[\frac{1}{E(k)} \frac{\partial E(k)}{\partial a_y} + \frac{y^2}{a_y^3 \alpha} \right]^{-1} \right\} \tag{B.7}$$

The functions g_1 and g_2, defined in Equation (A.9) may be determined by stress analysis of both the solution geometry and the reference geometry using some least-square fit to determine these functions in terms of a_x and a_y.

The methodology given in this appendix has been applied in (11) to solve the two DOF quarter-ellipse corner crack from only twelve full, three-dimensional, boundary-integral equation stress analyses. Furthermore, the methods described here could easily be extended to problems with more than one or two DOF in order to solve much more complex geometries and loading states.

B.2 Estimation of h for Three-Dimensional Problems From Analogous Two-Dimensional Solutions

Lacking the tools and time to perform numerical three-dimensional stress analysis, three-dimensional h can sometimes be estimated from analogous two-dimensional h values. The estimated results may be in error and must be checked against known analytical and experimental results.

To illustrate a two-dimensional approximation, consider the elliptical surface and corner cracks in Fig. 7. The correct way to solve either of the problems in Fig. 7 is outlined above and performed in (11). However, an approximation was initially assessed to compute $\bar{K}$ for surface and corner cracks in infinite solids. Fig. 7 illustrates the applied procedure. The influence function due to Bueckner (20) for the two-dimensional surface crack in a semi-infinite plate is applied to each cartesian line of the elliptical crack that intersects a free surface.

For two-dimensional problems, Bueckner's equation may be rewritten as:

$$K_{2s} = \int_0^1 h_{2s}(\bar{x}, a)\, \sigma(\bar{x})\, d\bar{x} \qquad (B.8)$$

where:

$$h_{2s} = h_{2e}\, f_s(\bar{x})$$

h_{2s} = two-dimensional surface crack influence function

h_{2e} = two-dimensional internal crack influence function for $\sigma(\bar{x}) = \sigma(-\bar{x})$; given in (2.4)

K_{2s} = K-factor for two-dimensional surface crack for any $\sigma(\bar{x})$

$\bar{x} = x/a$

and $f_s(\bar{x}) = \sqrt{1 + \bar{x}}\,(1.3188 - .7884\bar{x} + .1768\bar{x}^2)$ (B.9)

By breaking up the surface and corner ellipses as shown in Fig. 7, inexact three-dimensional analogs to (B.8) may be constructed for the surface crack.

$$h_x^{(s)}(x,y,a_x,a_y) = 2h_x \quad f_s(x_s)$$
$$h_y^{(s)}(x,y,a_x,a_y) = 2h_y \quad f_s(x_s) \tag{B.10}$$

and for the corner crack

$$h_x^{(c)}(x,y,a_x,a_y) = 4h_x \quad \left[f_s(x_s) + f_s(y_s) - 1\right]$$
$$h_y^{(c)}(x,y,a_x,a_y) = 4h_y \quad \left[f_s(x_s) + f_s(y_s) - 1\right] \tag{B.11}$$

where

$$x_s = x/x_{max} = \frac{x}{a_x(1 - \bar{y}^2)^{1/2}}$$
$$y_s = y/y_{max} = \frac{y}{a_y(1 - \bar{x}^2)^{1/2}} \tag{B.12}$$

Equations (3.9, B.1, B.9 - B.12) are being used to estimate $\bar{K}_x$ and $\bar{K}_y$ for half-ellipse surface cracks and quarter-ellipse corner cracks. Table VI compares normalized local values of K, $\hat{K}$, with normalized $\hat{K}$ for several crack geometries under uniform stress. The differences between $\hat{K}$ and $\hat{K}$ follow expected trends. For example, for the embedded circle,

$$\hat{K}_y = \bar{K}_y = K_x = \hat{K}_y = 1 \tag{B.13}$$

For the surface cracks

$$\hat{K}_y > \bar{K}_y > K_x > \hat{K}_x \tag{B.14}$$

and this occurs, as expected. For the corner crack

$$\bar{K}_x = \bar{K}_y < \overset{\Lambda}{K}_x = \overset{\Lambda}{K}_y \tag{B.15}$$

since, as shown by (11), the K level is highest near the surface.

Perusal of K and $\bar{K}$ results (11,28) for various points on the circular periphery indicates that the $\bar{K}$ values computed here for surface cracks are too high. The errors are up to 5% for the circular crack and less for ellipses with b/a > 1.

For the elongated ellipse (b/a → ∞) the surface correction is expected to increase $\bar{K}_x$ by about 13% as for the two-dimensional crack. Table VI shows this expected trend.

APPENDIX C

THE FOUR-DOF BURIED ELLIPTICAL CRACK

C.1 Introduction

This report introduces a new technique for residual lifetime estimates for structures with part-through cracks. The notion of a set of stress intensity factors ($\bar{K}_i$) is introduced to predict crack growth rates. Each $\bar{K}_i$ is related to the strain energy release rate due to perturbation of only the ith crack dimension or degree-of-freedom (DOF).

This appendix presents the exact solution for the case of a four DOF embedded elliptical crack, described in Section 3.2.6 and Fig. 8, which allows selective axis growth and also allows x' and y' translation of the ellipse center.

A new computer code (IF3-1) has been written to use both the two and four DOF results given in the report.

C.2 Problem Description and Definition

The x' -y' origin is the initial center of the four-degree-of-freedom (4 DOF) buried elliptical crack in an infinite solid shown in Fig. 8. All four DOF (a_1, a_2, a_3, a_4) are measured from the x'-y' origin. The origin of the coordinate system (x,y) that moves with the ellipse is the current ellipse center as illustrated in Fig. 8. As shown, the ellipse dimensions are $2a_x$ and $2a_y$.

This kinematic description in terms of two coordinate systems is very useful. This is true because it is obvious that under the applied reference uniform stress field $\sigma^*(x,y) = \sigma_o$, the crack opening displacement (COD) field

is a function of only σ_o, a_x, a_y, x, and y.

The COD function for the upper crack face is given in Appendix B as

$$w = \frac{2\,\sigma_o\,a_x}{HE(k)}\,\alpha^{\frac{1}{2}} \tag{C.1}$$

Expressions for $\bar{K}_i^*$, h_i, and $\bar{K}_i$ (i = 1, 4) are now derived. These are the reference (uniform stress) root mean square (rms) stress intensity (K) factors, the influence functions, and the general rms K-factors.

C.3 The $\bar{K}_i^*$ Computation

From Section 3,

$$\bar{K}_i^* = (H\,G_i^*)^{\frac{1}{2}} \tag{C.2}$$

where the asterisk denotes the reference condition and the strain energy release rate is

$$G_i^* = \frac{\partial U^*}{\partial a_i}\,\frac{\partial a_i}{\partial A} \tag{C.3}$$

and where the ellipse area is a $A = \pi a_x\,a_y = \frac{\pi}{4}\,(a_1 + a_2)\,(a_3 + a_4)$, and the strain energy is

$$U^* = \int_A \sigma_o\,w^*\,dA. \tag{C.4}$$

By inspection, a perturbation of a_1 will open half the new area and release half the strain energy that would equal perturbation of a_x. That is

$$\frac{\partial a_1}{\partial A} = 2\,\frac{\partial a_x}{\partial A} = \frac{2}{\pi a_y} \tag{C.5}$$

$$\frac{\partial U^*}{\partial a_1} = \frac{1}{2} \frac{\partial U^*}{\partial a_x} \tag{C.6}$$

Thus, combination of (C.3), (C.5), and (C.6) gives

$$\bar{K}_1^* = \bar{K}_x^* \tag{C.7}$$

$$\bar{K}_2^* = \bar{K}_x^* \tag{C.8}$$

and

$$\bar{K}_3^* = \bar{K}_4^* = \bar{K}_y^* \tag{C.9}$$

where $\bar{K}_x^*$ and $\bar{K}_y^*$ are derived by setting $\sigma_{zz}(x, y) = \sigma_o$ in Equation (3.6) in Section 3, obtaining

$$\bar{K}_x^* = 2\sigma_o \sqrt{a_x} \left[\frac{1}{3E(k)} \left(\frac{2}{a_x} - \frac{\partial E(k)}{E(k)\, \partial a_x} \right) \right]^{\frac{1}{2}} \tag{C.10}$$

$$\bar{K}_y^* = 2\sigma_o \left[\frac{a_x a_y}{E(k)} \left(\frac{1}{a_y} - \frac{\partial E(k)}{E(k)\, \partial a_y} \right) \right]^{\frac{1}{2}} \tag{C.11}$$

C.4 The Computation of Influence Functions h_i

The basic formula for influence functions is given in Section 3 and the influence function for some point (x', y') in the fixed coordinate system, may be expressed as

$$h_1(a_i, x', y') = \frac{H}{\bar{K}_1^*} \frac{\partial w^*}{\partial a_1} \frac{\partial a_1}{\partial A} \tag{C.12}$$

Since w* depends only on σ_o, a_x, a_y, x, and y, it is advantageous to express $\frac{\partial w^*}{\partial a_1}$ in terms of $\frac{\partial w^*}{\partial a_x}$. From Fig. 8,

$$a_1 = a_x - x + x' \tag{C.13}$$

$$a_1 = 2a_x - a_2 \tag{C.14}$$

The differentials of (C.13) and (C.14) are

$$da_1 = da_x - dx + dx' \qquad (dx' \equiv 0) \tag{C.15}$$

$$da_1 = 2da_x - da_2 \qquad (da_2 \equiv 0) \tag{C.16}$$

where dx' is zero because the reference point is fixed in the stationary x'-y' coordinate system in terms of which the stress fields $\sigma(x', y')$ are defined. The term da_2 is zero because $\bar{K}_1^*$ and h_1 are quantities resulting from the perturbation of only the first freedom. The solution of (C.15) and (C.16) is

$$\frac{\partial a_x}{\partial a_1} = -\frac{\partial x}{\partial a_1} = \tfrac{1}{2} \tag{C.17}$$

Application of the chain rule and (C.17) yields

$$\frac{\partial w^*}{\partial a_1} = \tfrac{1}{2}\left(\frac{\partial w^*}{\partial a_x} - \frac{\partial w^*}{\partial x}\right) \tag{C.18}$$

where the partial derivatives of (C.1) are

$$\frac{\partial w^*}{\partial a_x} = w^*(x, y, a_x, a_y)\left(\frac{1}{a_x} - \frac{\partial E(k)}{E(k)\,\partial a_x} + \frac{x^2}{a_x^3\,\alpha}\right) \tag{C.19}$$

and

$$\frac{\partial w^*}{\partial x} = \frac{-w^* x}{a_x^2 \alpha} \tag{C.20}$$

Combining (C.18 - C.20), we obtain

$$\frac{\partial w^*}{\partial a_1} = \frac{a_x \sigma_0 \alpha^{1/2}}{HE(k)} \left[\frac{1}{a_x} - \frac{\partial E(k)}{E(k)\,\partial a_x} + \frac{x}{a_x^2 \alpha} \left(\frac{x}{a_x} + 1 \right) \right] \tag{C.21}$$

Combination of (C.5), (C.10), (C.12) and (C.21) gives the influence function for the first freedom. Similar developments lead to similar expressions for the second, third and fourth freedoms, i=2,4. All h_i are given by the following expressions.

$$h_{\substack{1 \\ 2}} = \frac{\alpha^{1/2} \left[\frac{1}{a_x} - \frac{\partial E(k)}{E(k)\partial a_x} + \frac{x}{a_x^2 \alpha} \left(\frac{x}{a_x} \pm 1 \right) \right]}{\pi a_y \left[\frac{E(k)}{3} \left(\frac{2}{a_x} - \frac{\partial E(k)}{E(k)\partial a_x} \right) \right]^{1/2}} \tag{C.22}$$

$$h_{\substack{3 \\ 4}} = \frac{\alpha^{1/2} \left[\frac{-\partial E(k)}{E(k)\,\partial a_y} + \frac{y}{a_y^2 \alpha} \left(\frac{y}{a_y} \pm 1 \right) \right]}{\pi \left[\frac{a_x a_y E(k)}{3} \left(\frac{1}{a_y} - \frac{\partial E(k)}{E(k)\,\partial a_y} \right) \right]^{1/2}} \tag{C.23}$$

C.5 The Computation of Stress Intensity Functions for Completely General Stress Field $\sigma(x',y')$

The $\bar{K}_i$, i=1,4 computations follow immediately from the definition of the h_i as given in Section 3 and Appendix B. The result is

$$\bar{K}_i = \iint_A h_i\,(a_x, a_y, x, y)\ \sigma(x',y')\ dxdy \qquad (C.24)$$

where

$$x' = x + a_1 - a_x$$

$$y' = y + a_3 - a_y$$

APPENDIX D

Listing of Computer Program IF2-1, Data Listing and Results of the Six Weld Crack Fatigue Analyses of Table IV.

```
$WATFIV
      REAL KTH,KIC,KRIG,M,N,L,KI,IF
      DIMENSION Z(50),X(100),DX(100),DDN(8),L(8),  C(10),B(6)
      SPY=0.7979645
   17 FN=0.
      SUM=0.
      READ(5,25) (Z(I),I=1,20)
   25 FORMAT(20A4)
      WRITE(6,60)
   60 FORMAT(///)
      WRITE(6,25) (Z(I),I=1,20)
      READ(5,1,END=1000) L(1)
      WRITE(6,21) L(1)
   21 FORMAT(/,24H THE INITIAL CRACK LENGTH IS,F10.5)
    1 FORMAT(8E10.5)
      READ(5,1)(C(I),I=1,6)
      READ(5,1) C(7),C(8)
      READ(5,1) C(9),C(10)
      WRITE (6,104)
  104 FORMAT(/'      DELTA SIGMA          MEAN SIGMA    EFFECTIVE FRACTI
     1ON OF RESIDUAL STRESS    HALF PLATE WIDTH   ' )
      WRITE (6,105) C(10), C (7), C(9),C(1)
  105 FORMAT (2020.5,15X, 2020.5)
      L(2)=L(1)
      READ(5,1) O,M,KTH,KIC
      READ(5,1)FINKX,CIN
      WRITE(6,40)
   40 FORMAT(/10X,'THE CRACK GROWTH RELATION IS:DA/DN=C*(KIEFFECTIVE-KTH
     1)**M/(KIC*(1.-RFRR)-KIEFFECTIVE)**')
      WRITE(6,41)
   41 FORMAT (09X,'THE CONSTANT''S VALUES ARE:   C          M          KTH
     1      KIC')
      WRITE(6,2) O,M, KTH, KIC
      WRITE(6,42) FINKX
      WRITE(6,43) CIN
   42 FORMAT(/5IH THE NUMBER OF INTEGRATION POINTS TO COMPUTE K-FACTORS
     1IS,F5.0)
   66 FORMAT( 71H THE NUMBER OF LIFE INTEGRATION POINTS TO DOUBLE THE CR
     1ACK DIMENSION IS,F6.0)
      READ (5,1)H
      IF(H).1
      IF(IH-3) 44,45,46
   44 WRITE(6,47) H
      GOTO 50
   45 CONTINUE
      GO TO 50
   46 WRITE(6,49) H
   50 CONTINUE
   47 FORMAT(/59H THE STRAIN ENERGY RELEASE RATE CRITERION WAS USED WITH
     1 F=,F5.2)
   48 FORMAT(/41H THE VON-MISES CRITERIA WAS USED WITH F= F5.2)
   49 FORMAT(/52H THE MAXIMUM SHEAR STRESS CRITERION WAS USED WITH F=,F5
     1.2)
   43 FORMAT(/' THE MULTI-MODE K-ESTIMATION EQUATION IS: KIEFFECTIVE =
     1SQRT(KI**2+O**(II I**2) ')
      CIN=2.**(1./(CIN-.0001))
    2 FORMAT(33X,4G10.3)
      INKX=FINK+.1
      DO 3 I=1,INKX
      F=I-.5
```

Initial Input/Output Including Extra Format Statements for Other (e.g. Multi-mode) Applications.

```
      F=F/FINK)
    3 X(I)=F* (2.-F)
      IXM=INKX-1
      DO 4 I=2, IXM
    4 DX(I)=(X(I+1)-X(I-1))/2.
      DX(1)=(X(1)+X(2))/2.
      DX(INKX)=1.-(X(INKX)+X(IXM))/2.
      W=C(1)
      WRITE(6,60)
      WRITE(6,30)
      WRITE(6,31)
      WRITE(6,32)
    5 FORMAT (/,8X,F20.7)
      WINK=W/INKX
      DO 6 I=1,INKX
      XP=(I-.5)* WINK
      CALL THICK(XP,TCALC,C)
    6 SUMW=SUMW+TCALC* WINK
      DO 8  IA=1, 100
      A=L(2)
      SUMA=0.
      SUMK=0.
      SKMIN=0
      SMKIII=C.
      AINK=A/INKX
      DO 9  I=1,INKX
      XP=(I-.5)*AINK
      CALL THICK(XP,TCALC,C)
    9 SUMA=SUMA+TCALC*AINK
      F=SUMA/SUMW
      DO 7 I=1,INKX
      XP=X(I)
      XPA=XP*A
      CALL THICK(XPA,TCALC,C)
      CALL STLIN (S,SKY,XPA,C)
      RBC=A/R
      PINT =    HCS(RE,A,XPA,1)*TCALC*C(10)*DX(I)
      SKMIN=SKMIN   +   PINT / C(10)* (S+C(2))
    7 SUMK=SUMK+PINT
      CALL THICK(A,T,C)
      ZZ=SUMK/T*A
      SKIII=SMKIII/T*A
      KI=ZZ**2+H *SKIII**2
      KI=SQRT(KI)
      SKMIN=SKMIN/T*A
      SKMAX=SKMIN + KI
      QZZM=C(5)*ZZ*.1
      QK3M=C(6)*SKIII
      QKIM=QZZM**2+H *QK3M**2
      QKIM=SQRT(QKIM)
      IF(SUMK+SKMIN) 101,101,102
  101 WRITE (6,103)
  103 FORMAT(/  '  CRACK HAS ARRESTED; LIFE IS INFINITE ' )
      GO TO 17
  102 CONTINUE
      RE=SKMIN/(SUMK + SKMIN)
      QKIX=KI
      KI=QKIX+QKIM
      QDK1=ZZ-QZZM
      QDK3=SKIII-QK3M
```

Break-up for Numerical Integration of

$$K = \int_{L_a} h(x, a, \text{etc.})\ \sigma(x)\ t(x)\ dx$$

Effective Width, Variable Thickness Calculations

ΔK Integration

K_{min} Integration

$\frac{da}{dN} \longrightarrow 0$ for $K_{max} \leq 0$

$R = K_{min}/K_{max}$

```
      DADN=C*(KI-KTH)**N/(KIC*(1.-RE )-KI)        <------ "Forman's Rule"  da/dN Relation
      IF(KI-KTH) 10,10,11
   10 DADN=0.
C  KI CHECKS
   11 IF (LKIX-KIC) 12,12,13
   13 DADN=-100.*DADN
      SPY=5.
   12 DDN(I)=DADN
      CALL INT(IA,CIN,FN,L,DDN)
      CALL STLIN ( S,SXY,A,C)
      CALL THICK(A,T,C)
   30 FORMAT('     CRACK          RESIDUAL STRESS       THICKNESS
     1  STRESS INTENSITY FACTORS    EFFECTIVE     CYCLIC CRACK     CYCLIC')
   31 FORMAT('     DEPTH          AXIAL          SHEAR                KMAX
     1KMIN         DELTA  K         KMIN/KMAX    GROWTH RATE       LIFE')
   32 FORMAT('       A          SXX(A)          SAY(A)       T(A)        KMAX
     1  KMIN          KMAX-KMIN        REFF            DA/DN            N  ')
      WRITE(6,33) L(1),S,SXY,T,SKMAX,SRKMIN,KI,RE,DADN,FN
   33 FORMAT(F11.5, F10.2, F14.2, F10.5,2F10.2,F16.2,F17.3,E16.3,F10.0)
      IF(L(2)-K) 19,19,13
   19 CONTINUE
   15 FORMAT(F20.7,F10.5,E15.5,2E15.5,2F25.1)
C  BREAK
      IF (SPY-1.) 8,8,18
    8 CONTINUE
   18 WRITE(6,16)
   16 FORMAT(/52H RUN TERMINATED-FRACTURE TOUGHNESS HAS BEEN EXCEEDED)
      SPY=0.7573345
      GO TO 17
 1000 STOP
      END
```

```
      SUBROUTINE INTEGA(A,CIN,FN,L,DDN)
      REAL L
      DIMENSION L(2),DDN(2)
      IF (IA-1) 4,4,5
    5 DBIG=.5*(DDN(1)+DDN(2))
      FN=FN+DLBIG/DBIG
      L(1)=L(1)+CLAI
    4 DLBIG=L(1)*(1.-1.)
      DDN(2)=DDN(1)
      L(2)=L(1)+CLAI
      RETURN
      END
```

Integrates $N(a) = \int_{a_i}^{a} \frac{da}{[da/dN]}$

with Trapizoidal Rule

Variable Thickness

```
      FUNCTION MCS(B,A,C,IMODE)
C
C             INFLUENCE FUNCTIONS FOR CENTER CRACK OF LENGTH 2A IN
C           PLATE OF WIDTH 2B UNDER SYMMETRIC MODE IMODE (=1,2, OR 3)
C           LOADING.          SOURCE: PAGE 2.34 OF TADA HANDBOOK.
C           ERROR: LESS THAN 1% FOR IMODE=1,2; EXACT FOR IMODE=3.
C           PROGRAMMER:  PHIL RESNER, MARCH 1975
C
      PCT=.2+67174
      PI2= 1.5707963
      PA=PI2*A/B
      PC=PI2*C/B
C               IS PA TOO SMALL FOR TRIGONOMETRIC FUNCTIONS?
      IF(PA-.016)1,1,2
    1 F3=PA/(PA*PA-PC*PC)* (1-PC*PC)
      MCS=SQRT(F3)
C               IF WE ARE IN MODE III, THE CALCULATION IS FINISHED
      GOTO (3,3,4),IMODE
    3 F1= 1+PCT*SQRT(1-C/A*C/A) *PA*PA/2
      MCS = MCS*F1
      GO TO 4
    2 TA=TAN(PA)
      CA=COS(PA)
      CC=COS(PC)
      CACC=CA/CC
      F3=TA/(1-CACC**2)
      MCS=SQRT(F3)
C               IF WE ARE IN MODE III, THE CALCULATION IS FINISHED
      GO TO (5,5,4),IMODE
    5 F1= 1 + PCT * SQRT(1-C/A*C/A) * (1.-CA)
      MCS=MCS*F1
    4 MCS=1.4142135*MCS/SQRT(B)
      RETURN
      END
```

Influence Function Subroutine; to be Changed for Each General 2-D Problem Class.

```
      SUBROUTINE   SPLIN(S,SXY,X,C)
      DIMENSION CS(50),CX(50),DS(50),DX(50) C(20)
      IF(C(6)-12000.) 1,1,2
    1 READ(5,3) IN
    3 FORMAT(I5)
      READ(5,4) (CX(I),CS(I),  I=1,IN)
    4 FORMAT(2F10.0)
      C(6)=12000.
      DO 5 I=2,IN
      DS(I)=CS(I)-CS(I-1)
    5 DX(I)=CX(I)-CX(I-1)
    2 CONTINUE
      DO 7 I=1,IN
      DI=X-CX(I+1)
      J=I
      IF (DI) 6,6,7
    7 CONTINUE
    6 S=CS(J)    +   DS(J+1) / DX(J+1)   * ( X - CX(I)    )
      S = C(6) = S
      SXY = 0.
      RETURN
      END
```

Linear Interpolation of σ_{res} (x) Function

Which is Input as a "Table."

```
229.     $DATA
230.        THRU-CRACK IN A WELD UNDER NOMINAL AND RESIDUAL STRESS
231.     .125003                                   <- a_i
232. t = 1000.       0.                           <- σ_min
233.     1.
234.     1.          2.                           <- Δσ
235.        1.4E-07  2.74                         <- n        150.  <- K_Ic
236.     30.         5.
237.     3.
238.     00015
239.                 52.5
240.     .4          50.
241.     .8          45.
242.     1.2         32.5
243.     1.6         19.
244.     1.8         14.
245.     2.4         7.
246.     3.          2.8
247.     3.6         0.
248.     4.5         -2.
249.     5.5         -2.8
250.     7.          -3.2
251.     20.         -7.
252.     27.5
253.     1000000.
254.        THRU-CRACK IN A WELD UNDER NOMINAL AND RESIDUAL STRESS
255.     .125003
256.     1000.       -30.
257.     1.
258.     1.          25.
259.        1.4E-07  2.74                         150.
260.     30.         5.
261.     3.
262.     00015
263.                 52.5
264.     .4          50.
265.     .8          45.
266.     1.2         32.5
267.     1.6         19.
268.     1.8         14.
269.     2.4         7.
270.     3.          2.8
271.     3.6         0.
272.     4.5         -2.
273.     5.5         -2.8
274.     7.          -3.2
275.     20.         -7.
276.     27.5
277.     1000000.
278.        THRU-CRACK IN A WELD UNDER NOMINAL AND RESIDUAL STRESS
279.     .125003
280.     5.
281.     1.
282.     1.          25.
283.        1.4E-07  2.74                         150.
284.     30.         5.
285.     3.
286.     00011
287.                 52.
```

Residual Stress Table for

$\sigma_{res}(x) = \sigma_{res}(-x)$

Lines 230-366

Input Data for Six Fatigue Analyses of Table IV.

```
288.      .4          48.5
289.      .8          44.
290.      1.2         40.
291.      1.6         7.5
292.      1.8         3.7
293.      2.4         -9.
294.      3.          -17.
295.      3.6         -22.
296.      4.5         -35.5
297.      5.5         -37.5
298.         THRU-CRACK IN A WELD UNDER NOMINAL AND RESIDUAL STRESS
299.      .125003
300.      5.          -30.
301.      1.
302.      1.          25.
303.         1.4E-072.74                 150.
304.      30.         5.
305.      3.
306.      00011
307.                  52.
308.      .4          48.5
309.      .8          38.
310.      1.2         20.
311.      1.6         7.5
312.      1.8         3.7
313.      2.4         -9.
314.      3.          -17.
315.      3.6         -22.
316.      4.5         -35.5
317.      5.5         -37.5
318.         THRU-CRACK IN A WELD UNDER NOMINAL AND RESIDUAL STRESS
319.      .125003
320.      1000.       0.
321.      1.
322.      0.          25.
323.         1.4E-072.74                 150.
324.      30.         5.
325.      3.
326.      00015
327.                  52.5
328.      .4          50.
329.      .8          45.
330.      1.2         32.5
331.      1.6         19.
332.      1.8         14.
333.      2.4         7.
334.      3.          2.8
335.      3.6         0.
336.      4.5         -2.
337.      5.5         -2.8
338.      7.          -3.2
339.      20.         -7.
340.      27.5
341.      1000000.
342.         THRU-CRACK IN A WELD UNDER NOMINAL AND RESIDUAL STRESS
343.      .125003
344.      5.          0.
345.      1.
346.      0.          25.
347.         1.4E-072.74                 150.
```

```
348.      30.         5.
349.      3.
350.      00015
351.                  52.5
352.      .4          50.
353.      .8          45.
354.      1.2         32.5
355.      1.6         17.
356.      1.8         14.
357.      2.4         7.
358.      3.          3.8
359.      3.6         0.
360.      4.5         -2.
361.      5.5         -2.8
362.      7.          -3.2
363.      20.         -7.
364.      27.5
365.      1000000.
366.
367.      $STOP
```

$DATA

THRL-CRACK IN A WELD UNDER NOMINAL AND RESIDUAL STRESS - Case 1

THE INITIAL HALF CRACK LENGTH IS 0.12500

DELTA SIGMA	MIN SIGMA	EFFECTIVE FRACTION OF RESIDUAL STRESS	HALF PLATE WIDTH
25.000	0.00000	1.0000	(1000.0)

← Large Pipe ≈ Infinite Plate

THE CRACK GROWTH RELATION IS: DA/DN=C*(KIEFFECTIVE-KTH)**M/((KIC*(1.-REFF)-KIEFFECTIVE)

THE CONSTANTS VALUES ARE:

C	M	KTH	KIC
0.140E-06	2.74	0.000	150.

THE NUMBER OF INTEGRATION POINTS TO COMPUTE K-FACTORS IS 30.
THE NUMBER OF LIFE INTEGRATION POINTS TO DOUBLE THE CRACK DIMENSION IS 5.

HALF CRACK LENGTH A	RESIDUAL STRESS AXIAL SXX(A)	RESIDUAL STRESS SHEAR SXY(A)	THICKNESS T(A)	STRESS INTENSITY FACTORS KMAX	STRESS INTENSITY FACTORS K MIN KMIN	STRESS INTENSITY FACTORS DELTA K KMAX-KMIN	EFFECTIVE KMIN/KMAX REFF	CYCLIC CRACK GROWTH RATE DA/DN	CYCLIC LIFE N
0.12500	51.72	0.00	1.00000	48.60	32.82	15.78	0.675	0.816E-05	0.
0.14355	51.60	0.00	1.00000	52.04	35.13	16.91	0.675	0.102E-04	2026.
0.16494	51.47	0.00	1.00000	55.71	37.59	18.13	0.675	0.128E-04	3883.
0.18947	51.32	0.00	1.00000	59.64	40.21	19.43	0.674	0.161E-04	5579.
0.21764	51.14	0.00	1.00000	63.82	43.00	20.82	0.674	0.204E-04	7121.
0.25001	50.94	0.00	1.00000	68.29	45.97	22.32	0.673	0.260E-04	8516.
0.28718	50.71	0.00	1.00000	73.05	49.13	23.92	0.673	0.333E-04	9770.
0.32989	50.44	0.00	1.00000	78.12	52.48	25.63	0.672	0.430E-04	10939.
0.37894	50.13	0.00	1.00000	83.51	56.03	27.48	0.671	0.561E-04	11879.
0.43525	49.76	0.00	1.00000	89.19	59.74	29.45	0.670	0.739E-04	12746.
0.50002	48.75	0.00	1.00000	95.09	63.53	31.56	0.668	0.984E-04	13497.
0.57438	47.62	0.00	1.00000	101.25	67.43	33.83	0.666	0.133E-03	14139.
0.65975	46.75	0.00	1.00000	107.65	71.39	36.25	0.663	0.174E-03	14678.
0.75790	45.53	0.00	1.00000	114.26	75.40	38.85	0.660	0.261E-03	15119.
0.87006	42.74	0.00	1.00000	120.66	79.02	41.64	0.655	0.379E-03	15472.
1.00005	38.75	0.00	1.00000	126.13	81.50	44.63	0.646	0.549E-03	15751.
1.14876	34.10	0.00	1.00000	130.70	82.87	47.83	0.634	0.794E-03	15972.
1.31958	28.46	0.00	1.00000	134.04	82.77	51.27	0.618	0.111E-02	16152.
1.51580	21.84	0.00	1.00000	135.65	80.70	54.95	0.595	0.141E-02	16337.
1.74121	15.47	0.00	1.00000	135.59	76.70	58.89	0.566	0.158E-02	16458.
2.00012	11.67	0.00	1.00000	135.48	72.36	63.12	0.534	0.177E-02	16612.
2.29754	8.20	0.00	1.00000	135.55	67.90	67.65	0.501	0.201E-02	16770.
2.63919	5.33	0.00	1.00000	135.41	62.91	72.51	0.465	0.224E-02	16930.
3.03164	2.65	0.00	1.00000	135.27	57.55	77.72	0.425	0.250E-02	17096.
3.48244	0.55	0.00	1.00000	135.24	51.95	83.29	0.384	0.282E-02	17265.
4.00028	-0.39	0.00	1.00000	135.50	46.23	89.27	0.341	0.324E-02	17436.
4.59513	-2.08	0.00	1.00000	136.26	40.59	95.67	0.298	0.386E-02	17603.
5.27843	-2.62	0.00	1.00000	137.98	35.44	102.54	0.257	0.507E-02	17756.
6.06333	-2.95	0.00	1.00000	140.39	30.49	109.90	0.217	0.728E-02	17883.
6.96455	-3.19	0.00	1.00000	143.74	25.95	117.79	0.181	0.129E-01	17972.
8.00065	-3.49	0.00	1.00000	147.79	21.55	126.24	0.146	0.424E-01	(18009.)

RUN TERMINATED-FRACTURE TOUGHNESS HAS BEEN EXCEEDED

THRU-CRACK IN A WELD UNDER NOMINAL AND RESIDUAL STRESS – Case 2, Negative Applied σ

THE INITIAL HALF CRACK LENGTH IS 0.12500

DELTA SIGMA	MIN SIGMA	EFFECTIVE FRACTION OF RESIDUAL STRESS	HALF PLATE WIDTH
25.000	-30.000	1.0000	1000.0

THE CRACK GROWTH RELATION IS:DA/DN=C*(KIEFFECTIVE-KTH)**M/((1.-KIC*(1.-REFF)-KICEFFECTIVE)

THE CONSTANTS VALUES ARE: C M KTH KIC

0.140E-08 2.74 0.000 150.

THE NUMBER OF INTEGRATION POINTS TO COMPUTE K-FACTORS IS 50.
THE NUMBER OF LIFE INTEGRATION POINTS TO DOUBLE THE CRACK DIMENSION IS 5.

HALF CRACK	RESIDUAL STRESS AXIAL	RESIDUAL STRESS SHEAR	THICKNESS	STRESS INTENSITY FACTORS KMAX	STRESS INTENSITY FACTORS KMIN	STRESS INTENSITY FACTORS DELTA K	EFFECTIVE KMIN/KMAX	CYCLIC CRACK GROWTH RATE	CYCLIC LIFE
A	SXX(A)	SXY(A)	T(A)	KMAX	KMIN	KMAX-KMIN	REFF	DA/DN	N
0.12500	51.72	0.00	1.00000	25.67	13.89	11.78	0.448	0.419E-05	0.
0.14359	51.60	0.00	1.00000	31.75	16.82	14.91	0.447	0.515E-05	3977.
0.16454	51.47	0.00	1.00000	33.96	15.84	18.13	0.466	0.634E-05	7693.
0.18947	51.32	0.00	1.00000	36.32	16.90	19.43	0.465	0.781E-05	11151.
0.21764	51.14	0.00	1.00000	38.84	18.02	20.82	0.464	0.963E-05	14392.
0.25001	50.94	0.00	1.00000	41.51	19.19	22.32	0.462	0.119E-04	17379.
0.28718	50.71	0.00	1.00000	44.34	20.43	23.92	0.461	0.147E-04	20191.
0.32989	50.44	0.00	1.00000	47.35	21.72	25.63	0.459	0.183E-04	22781.
0.37894	50.13	0.00	1.00000	50.54	23.06	27.49	0.456	0.227E-04	25177.
0.43539	49.78	0.00	1.00000	53.85	24.41	29.45	0.453	0.282E-04	27390.
0.50002	49.39	0.00	1.00000	57.27	25.64	31.63	0.448	0.351E-04	29435.
0.57436	47.93	0.00	1.00000	60.66	26.83	33.83	0.442	0.435E-04	31329.
0.65975	46.79	0.00	1.00000	64.14	27.99	36.15	0.436	0.540E-04	33079.
0.75760	46.53	0.00	1.00000	67.63	28.78	38.85	0.425	0.670E-04	34700.
0.87060	42.70	0.00	1.00000	70.69	29.04	41.64	0.411	0.821E-04	36212.
1.00005	38.75	0.00	1.00000	72.57	27.94	44.63	0.385	0.997E-04	37655.
1.14876	34.10	0.00	1.00000	73.30	25.47	47.83	0.347	0.112E-03	39075.
1.31958	28.46	0.00	1.00000	72.92	21.25	51.67	0.293	0.124E-03	40525.
1.51580	21.94	0.00	1.00000	69.71	14.76	54.95	0.212	0.130E-03	41974.
1.74121	15.47	0.00	1.00000	64.92	6.62	58.31	0.103	0.129E-03	43332.
2.00012	11.97	0.00	1.00000	59.73	-3.39	63.12	-0.057	0.126E-03	45351.
2.29754	8.20	0.00	1.00000	54.37	-13.29	67.65	-0.244	0.122E-03	48255.
2.63919	5.33	0.00	1.00000	48.41	-24.10	72.51	-0.498	0.115E-03	51149.
3.03164	2.69	0.00	1.00000	42.01	-35.70	77.72	-0.850	0.106E-03	54497.
3.48244	0.55	0.00	1.00000	35.29	-48.00	83.29	-1.360	0.946E-04	59183.
4.00028	-0.86	0.00	1.00000	28.38	-60.99	89.37	-2.149	0.810E-04	65087.
4.59513	-2.08	0.00	1.00000	21.46	-74.22	95.67	-3.459	0.653E-04	73219.
5.27843	-2.62	0.00	1.00000	14.53	-87.61	102.14	-5.867	0.485E-04	85130.
6.06333	-2.95	0.00	1.00000	8.51	-101.40	109.90	-11.921	0.300E-04	105117.
6.96495	-3.19	0.00	1.00000	2.29	-115.48	117.77	-48.234	0.911E-05	151278.

CRACK HAS ARRESTED; LIFE IS INFINITE ∞

THRU-CRACK IN A WELD UNDER NOMINAL AND RESIDUAL STRESS – Case 3

THE INITIAL HALF CRACK LENGTH IS 0.12500

DELTA SIGMA	MIN SIGMA	EFFECTIVE FRACTION OF RESIDUAL STRESS	HALF PLATE WIDTH
25.000	0.00000	1.0000	5.0000

10" Wide Specimen

THE CRACK GROWTH RELATION IS:DA/DN=C*(KIEFFECTIVE-KTH)**M/(KIC*(1.-REFF)-KIEFFECTIVE)

THE CONSTANT'S VALUES ARE:	C	M	KTH	KIC
	C.140E-06	2.74	C.000	150.

THE NUMBER OF INTEGRATION POINTS TO COMPUTE K-FACTORS IS 30.
THE NUMBER OF LIFE INTEGRATION POINTS TO DOUBLE THE CRACK DIMENSION IS 5.

HALF CRACK	RESIDUAL STRESS		THICKNESS	STRESS INTENSITY FACTORS			EFFECTIVE	CYCLIC CRACK	CYCLIC
	AXIAL	SHEAR		KMAX	K MIN	DELTA K	KMIN/KMAX	GROWTH RATE	LIFE
A	SXX(A)	SXY(A)	T(A)	KMAX	KMIN	KMAX-KMIN	REFF	DA/DN	N
0.12500	50.91	0.00	1.00000	47.97	32.25	15.72	0.672	C.794E-05	0.
0.14359	50.74	0.00	1.00000	51.43	34.55	16.87	0.672	C.997E-05	2075.
0.16454	50.56	0.00	1.00000	55.07	36.98	18.10	0.671	C.125E-04	3973.
0.16947	50.34	0.00	1.00000	55.03	39.60	19.43	0.671	C.159E-04	5700.
0.21754	50.10	0.00	1.00000	63.13	42.30	20.83	0.670	0.200E-04	7270.
0.25001	49.81	0.00	1.00000	67.59	45.24	22.35	0.669	0.256E-04	8689.
0.28719	49.49	0.00	1.00000	72.25	48.29	23.96	0.668	0.327E-04	9955.
0.32989	49.11	0.00	1.00000	77.26	51.56	25.70	0.667	0.422E-04	11105.
0.37894	48.68	0.00	1.00000	82.58	55.01	27.57	0.666	0.550E-04	12114.
0.43529	48.17	0.00	1.00000	88.13	58.54	29.59	0.664	0.724E-04	12998.
0.50002	45.57	0.00	1.00000	93.67	61.91	31.76	0.661	0.956E-04	13759.
0.57428	47.02	0.00	1.00000	99.27	65.16	34.11	0.656	C.127E-03	14436.
0.65979	41.65	0.00	1.00000	104.94	68.28	36.66	0.651	0.172E-03	15009.
0.75790	39.11	0.00	1.00000	110.60	71.17	39.43	0.643	0.235E-03	15490.
0.87060	34.82	0.00	1.00000	115.82	73.36	42.47	0.633	0.323E-03	15894.
1.00005	29.00	0.00	1.00000	119.84	74.03	45.80	0.618	C.432E-03	16237.
1.14876	22.81	0.00	1.00000	122.64	73.13	49.50	0.596	0.556E-03	16538.
1.31959	16.25	0.00	1.00000	124.59	70.94	53.66	0.569	0.702E-03	16809.
1.51560	10.12	0.00	1.00000	126.13	67.76	58.38	0.537	C.876E-03	17058.
1.74121	6.82	0.00	1.00000	127.35	63.50	63.85	0.499	C.109E-02	17287.
2.00012	-0.24	0.00	1.00000	128.06	58.04	70.03	0.455	0.140E-02	17495.
2.29754	-6.93	0.00	1.00000	130.27	52.01	78.26	0.399	0.182E-02	17679.
2.63919	-12.49	0.00	1.00000	132.44	44.06	88.39	0.333	0.257E-02	17835.
3.03164	-17.26	0.00	1.00000	137.43	35.30	102.15	0.257	C.480E-02	17941.
3.48244	-21.32	0.00	1.00000	149.31	26.58	122.74	0.178	0.132E 00	17968.
4.00028	-28.00	0.00	1.00000	174.96	15.45	159.51	0.088	0.668E 00	17969.

RUN TERMINATED-FRACTURE TOUGHNESS HAS BEEN EXCEEDED

THRU-CRACK IN A WELD UNDER NOMINAL AND RESIDUAL STRESS - Case 4

THE INITIAL HALF CRACK LENGTH IS 0.12500

DELTA SIGMA	MIN SIGMA	EFFECTIVE FRACTION OF RESIDUAL STRESS	HALF PLATE WIDTH
25.000	-30.000	1.0000	5.0000

THE CRACK GROWTH RELATION IS:DA/DN=C*(KIEFFECTIVE-KTH)**M/(KIC*(1.-REFF)-KIEFFECTIVE)

THE CONSTANT'S VALUES ARE:	C	M	KTH	KIC
	C.140E-06	2.74	0.000	150.

THE NUMBER OF INTEGRATION POINTS TO COMPUTE K-FACTORS IS 30.
THE NUMBER OF LIFE INTEGRATION POINTS TO DOUBLE THE CRACK DIMENSION IS 5.

CRACK DEPTH a	RESIDUAL STRESS AXIAL SXX(A)	RESIDUAL STRESS BEND SXX(A)	THICKNESS T(A)	KMAX KMAX	STRESS INTENSITY FACTORS K MIN	DELTA K KMAX-KMIN	EFFECTIVE KMIN/KMAX RATIO	CYCLIC CRACK GROWTH RATE DA/DN	CYCLIC LIFE N
0.12500	51.81	0.00	1.00000	25.11	13.39	11.72	0.460	0.407E-05	0.
0.14359	50.74	0.00	1.00000	31.18	14.31	16.87	0.459	0.502E-05	4092.
0.16434	49.58	0.00	1.00000	33.36	15.20	18.16	0.457	0.618E-05	7933.
0.18947	48.34	0.00	1.00000	35.71	16.28	19.43	0.456	0.764E-05	11458.
0.21764	47.10	0.00	1.00000	38.14	17.41	20.73	0.456	0.940E-05	14765.
0.24901	45.86	0.00	1.00000	40.77	18.42	22.35	0.452	0.116E-04	17862.
0.28371	44.60	0.00	1.00000	43.50	19.54	23.96	0.449	0.144E-04	20701.
0.32196	43.31	0.00	1.00000	46.42	20.72	25.70	0.446	0.178E-04	23354.
0.36404	42.00	0.00	1.00000	49.50	21.83	27.67	0.443	0.221E-04	25810.
0.41025	40.67	0.00	1.00000	52.62	23.03	29.59	0.438	0.275E-04	28093.
0.46092	39.32	0.00	1.00000	55.96	24.23	31.74	0.428	0.336E-04	30197.
0.51638	37.92	0.00	1.00000	59.36	24.23	34.11	0.415	0.414E-04	32174.
0.57695	36.48	0.00	1.00000	60.95	24.29	36.66	0.398	0.505E-04	34033.
0.75760	34.11	0.00	1.00000	63.29	23.85	39.43	0.377	0.611E-04	35791.
0.87060	34.52	0.00	1.00000	64.87	22.40	42.47	0.345	0.736E-04	37477.
1.00005	29.07	0.00	1.00000	64.87	19.07	45.80	0.294	0.885E-04	39144.
1.14874	27.51	0.00	1.00000	63.23	17.77	45.46	0.281	0.907E-04	40359.
1.31998	25.26	0.00	1.00000	60.20	8.55	51.66	0.100	0.960E-04	42689.
1.51560	10.13	0.00	1.00000	54.04	-2.30	56.38	-0.041	0.990E-04	44703.
1.74181	6.82	0.00	1.00000	50.73	-17.11	67.85	-0.338	0.550E-04	46980.
2.00012	-0.54	0.00	1.00000	44.57	-25.76	70.33	-0.578	1.969E-04	49624.
2.29764	-6.43	0.00	1.00000	36.36	-41.93	78.26	-1.152	1.8B3E-04	52836.
2.62919	-12.19	0.00	1.00000	26.38	-62.00	88.39	-2.350	0.729E-04	57078.
3.03164	-17.26	0.00	1.00000	14.96	-87.29	102.15	-5.876	0.692E-04	63555.
3.48244	-21.32	0.00	1.00000	2.03	-120.70	122.74	-59.410	0.339E-05	79519.

CRACK HAS ARRESTED; LIFE IS INFINITE ∞

51

THRU-CRACK IN A WELD UNDER NOMINAL AND RESIDUAL STRESS — Case 5

HE INITIAL HALF CRACK LENGTH IS 0.12500

DELTA SIGMA	MIN SIGMA	EFFECTIVE FRACTION OF RESIDUAL STRESS	HALF PLATE WIDTH
25.000	0.00000	0.00000	1000.0

No Residuals

THE CRACK GROWTH RELATION IS=DA/DN=C*(KEFFECTIVE-KTH)**M/(1.-R)**(1.-M)-(KEFFECTIVE)

THE CONSTANTS VALUES ARE C M KTH KIC

0.14E-06 2.74 0.000 [illegible].

HE NUMBER OF INTEGRATION POINTS TO COMPUTE K-FACTORS IS 30.
HE NUMBER OF LIFE INTEGRATION POINTS TO DOUBLE THE CRACK DIMENSION IS 0.

HALF CRACK a	RESIDUAL STRESS AXIAL SXX(A)	RESIDUAL STRESS BEND SXX(A)	THICKNESS T(A)	KMAX KMAX	STRESS INTENSITY FACTORS K MIN	DELTA K KMAX-KMIN	EFFECTIVE KMIN/KMAX RATIO	CYCLIC CRACK GROWTH RATE DA/DN	CYCLIC LIFE N
0.12500	0.00	0.00	1.00000	15.74	0.00	15.74	0.000	0.200E-05	0.
0.14359	0.00	0.00	1.00000	16.46	0.00	16.46	0.000	0.244E-05	8373.
0.16434	0.00	0.00	1.00000	17.13	0.00	17.13	0.000	0.298E-05	16258.
0.18947	0.00	0.00	1.00000	15.43	0.00	15.43	0.000	0.364E-05	23677.
0.21764	0.00	0.00	1.00000	20.82	0.00	20.82	0.000	0.444E-05	30652.
0.25001	0.00	0.00	1.00000	22.32	0.00	22.32	0.000	0.544E-05	37204.

0.28419	0.00	0.00	1.00000	23.92	0.00	23.92	0.000	0.660E-05	43354.
0.32586	0.00	0.00	1.00000	25.63	0.00	25.63	0.000	0.814E-05	49119.
0.37004	0.00	0.00	1.00000	27.48	0.00	27.48	0.000	0.100E-04	54518.
0.42529	0.00	0.00	1.00000	29.45	0.00	29.45	0.000	0.123E-04	59557.
0.50002	0.00	0.00	1.00000	31.56	0.00	31.56	0.000	0.151E-04	64234.
0.59498	0.00	0.00	1.00000	33.83	0.00	33.83	0.000	0.187E-04	68681.
0.69179	0.00	0.00	1.00000	36.25	0.00	36.25	0.000	0.231E-04	72775.
0.77196	0.00	0.00	1.00000	38.85	0.00	38.85	0.000	0.285E-04	76578.
0.87040	0.00	0.00	1.00000	41.64	0.00	41.64	0.000	0.354E-04	80104.
1.00004	0.00	0.00	1.00000	44.64	0.00	44.64	0.000	0.440E-04	83365.
1.14976	0.00	0.00	1.00000	47.84	0.00	47.84	0.000	0.549E-04	86373.
1.31459	0.00	0.00	1.00000	51.27	0.00	51.27	0.000	0.687E-04	89139.
1.49960	0.00	0.00	1.00000	54.95	0.00	54.95	0.000	0.862E-04	91673.
1.70121	0.00	0.00	1.00000	58.89	0.00	58.89	0.000	0.109E-03	93995.
2.00012	0.00	0.00	1.00000	63.12	0.00	63.12	0.000	0.136E-03	96094.
2.28779	0.00	0.00	1.00000	67.65	0.00	67.65	0.000	0.176E-03	97979.
2.63819	0.00	0.00	1.00000	72.51	0.00	72.51	0.000	0.226E-03	99678.
3.02164	0.00	0.00	1.00000	77.72	0.00	77.72	0.000	0.293E-03	101190.
3.48244	0.00	0.00	1.00000	83.29	0.00	83.29	0.000	0.384E-03	102521.
4.00028	0.00	0.00	1.00000	89.27	0.00	89.27	0.000	0.510E-03	103679.
4.59513	0.00	0.00	1.00000	95.67	0.00	95.67	0.000	0.684E-03	104671.
5.27843	0.00	0.00	1.00000	102.54	0.00	102.54	0.000	0.554E-03	105503.
6.06239	0.00	0.00	1.00000	109.90	0.00	109.90	0.000	0.137E-02	106180.
6.96499	0.00	0.00	1.00000	117.79	0.00	117.79	0.000	0.206E-02	106707.
8.00065	0.00	0.00	1.00000	126.24	0.00	126.24	0.000	0.337E-02	107098.
9.19035	0.00	0.00	1.00000	135.30	0.00	135.30	0.000	0.658E-02	107327.
10.56056	0.00	0.00	1.00000	145.01	0.00	145.01	0.000	0.192E-01	107438.
12.12015	0.00	0.00	1.00000	154.73	0.00	154.73	0.000	0.256E 01	107439.

RUN TERMINATED-FRACTURE TOUGHNESS HAS BEEN EXCEEDED

THRU-CRACK IN A WELD UNDER NOMINAL AND RESIDUAL STRESS - Case 6

THE INITIAL HALF CRACK LENGTH IS 0.12500

DELTA SIGMA	MIN SIGMA	EFFECTIVE FRACTION OF RESIDUAL STRESS	HALF PLATE WIDTH
25.000	0.00000	1.0000	5.0000

No Residuals

THE CRACK GROWTH RELATION IS:DA/DN=C*(KIEFFECTIVE-KTH)**M/(KIC*(1.-REFF)-KIEFFECTIVE)

THE CONSTANTS VALUES ARE:

C	M	KTH	KIC
0.140E-06	2.74	0.000	150.

THE NUMBER OF INTEGRATION POINTS TO COMPUTE K-FACTORS IS 30.
THE NUMBER OF LIFE INTEGRATION POINTS TO DOUBLE THE CRACK DIMENSION IS 5.

HALF CRACK	RESIDUAL STRESS AXIAL	RESIDUAL STRESS SHEAR	THICKNESS	STRESS INTENSITY FACTORS KMAX	KMIN	DELTA K	EFFECTIVE	CYCLIC CRACK GROWTH RATE	CYCLIC LIFE
A	SXX(A)	SXY(A)	T(A)	KMAX	KMIN	KMAX-KMIN	KMIN/KMAX REFF	DA/DN	N
0.12500	0.00	0.00	1.00000	15.72	0.00	15.72	0.000	0.198E-05	0.
0.14356	0.00	0.00	1.00000	16.87	0.00	16.87	0.000	0.242E-05	8449.
0.16464	0.00	0.00	1.00000	18.10	0.00	18.10	0.000	0.296E-05	16377.
0.18947	0.00	0.00	1.00000	19.43	0.00	19.43	0.000	0.364E-05	23907.
0.21764	0.00	0.00	1.00000	20.83	0.00	20.83	0.000	0.445E-05	30777.
0.25001	0.00	0.00	1.00000	22.35	0.00	22.35	0.000	0.546E-05	37312.
0.28713	0.00	0.00	1.00000	23.96	0.00	23.96	0.000	0.669E-05	43433.
0.32959	0.00	0.00	1.00000	25.70	0.00	25.70	0.000	0.822E-05	49143.

0.37854	0.00	0.00	1.00000	27.57	0.00	27.57	0.000	0.101E-04	54513.
0.43529	0.00	0.00	1.00000	29.59	0.00	29.59	0.000	0.125E-04	59439.
0.50002	0.00	0.00	1.00000	31.76	0.00	31.76	0.000	0.154E-04	64135.
0.57438	0.00	0.00	1.00000	34.11	0.00	34.11	0.000	0.191E-04	68435.
0.65939	0.00	0.00	1.00000	36.66	0.00	36.66	0.000	0.235E-04	72407.
0.75760	0.00	0.00	1.00000	39.43	0.00	39.43	0.000	0.299E-04	76060.
0.87000	0.00	0.00	1.00000	42.47	0.00	42.47	0.000	0.376E-04	79400.
1.00005	0.00	0.00	1.00000	45.80	0.00	45.80	0.000	0.478E-04	82433.
1.14976	0.00	0.00	1.00000	49.50	0.00	49.50	0.000	0.613E-04	85160.
1.31955	0.00	0.00	1.00000	53.66	0.00	53.66	0.000	0.757E-04	87583.
1.51560	0.00	0.00	1.00000	58.38	0.00	58.38	0.000	0.106E-03	89701.
1.74121	0.00	0.00	1.00000	63.85	0.00	63.85	0.000	0.144E-03	91511.
2.00012	0.00	0.00	1.00000	70.33	0.00	70.33	0.000	0.202E-03	93008.
2.29754	0.00	0.00	1.00000	78.26	0.00	78.26	0.000	0.301E-03	94190.
2.63919	0.00	0.00	1.00000	88.39	0.00	88.39	0.000	0.489E-03	95055.
3.03164	0.00	0.00	1.00000	102.15	0.00	102.15	0.000	0.936E-03	95605.
3.48244	0.00	0.00	1.00000	122.74	0.00	122.74	0.000	0.272E-02	95852.
4.00028	0.00	0.00	1.00000	159.51	0.00	159.51	0.000	0.160E 01	95852.

RUN TERMINATED-FRACTURE TOUGHNESS HAS BEEN EXCEEDED

CORE USAGE OBJECT CODE= 9880 BYTES,ARRAY AREA= 2012 BYTES,TOTAL AREA AVAILABLE= 196680 BYTES

COMPILE TIME= 0.80 SEC,EXECUTION TIME= 20.61 SEC, WATFIV - VERSION 1 LEVEL 1 JANUARY 1970 DATE= 75/397

R A L P H S Y S T E M L O G

```
R  1.45.04 JOB 1265 -- STEP1    -- BEGINNING EXEC - PART 6 - CLASS Q
R  1.46.11 JOB 1265 END EXECUTION.


 -- STANFORD HIGH SPEED BATCH MONITOR --
//STEP1  JOB 'C768,318,002.5,,',"PHIL"                          JOB 1265
***SERVICE CLASS=Q EXEC=S PRINT=H                               ***RALPH
***SERVICE CLASS=Q                                              ***RALPH
// EXEC WATFIV
//GO.SYSIN DD *
//
          NORMAL JOB END


 RALPH JOB STATISTICS --    369 CARDS READ --      563 LINES PRINTED --      0 CARDS PUNCHED --    0.36 MINUTES EXECUTION TIME
                         0.36 MINUTES CPU TIME    0.00 MINUTES WAIT TIME       11 TOTAL I/O COUNT

EXECUTION CHARGED AT WEEKEND RATES

PRINTING  CHARGED AT WEEKEND RATES
```

REFERENCES

1. Bueckner, H.F., Transactions of the ASME, Aug. 1958, pp. 1226-1230.

2. Emery, A.F., Walker, G.E. and Williams, J.A., Journal of Basic Engineering, Dec. 1969, pp. 618 - 624.

3. Paris, P.C., Gomez, M. P. and Anderson, W.E., "A Rational Analytic Theory of Fatigue," The Trend in Engineering, Vol. 13, No. 1, University of Washington (January 1961).

4. Bueckner, H.F., Z. angew. Math. Mech., 1970, p. 529.

5. Bueckner, H.F., Chapter V of Methods of Analysis and Solutions of Cracks Problems, Ed. by G. C. Sih, Nordhoff, 1973.

6. Tada, H., Paris, P., and Irwin, G., "The Stress Analysis of Cracks Handbook," Del Research Corporation, 1973.

7. Bueckner, H.F., "Weight Functions for the Notched Bar," General Electric Report No. 69-LS-45 (1969).

8. Labbens, R.Pellissier-Tanon, A. and Heliot, J., "Practical Method for Calculating Stress-Intensity Factor Through Weight Functions," paper presented at the 8th National Symposium on Fracture Mechanics at Brown University (August 1974).

9. Rice, J.R., "Some Remarks on Elastic Crack-Tip Stress Fields," Int. J. Solids & Structures, Vol. 8, pp. 751-758, (1972).

10. Besuner, P.M., "Residual Life Estimates for Structures with Partial Thickness Cracks," ASTM Eighth National Symposium on Fracture Mechanics (May 1974), accepted for ASTM Publication (1975).

11. Cruse, T.A. and Besuner, P.M., "Residual Life Prediction for Surface Cracks in Complex Structural Details," Symposium on Propulsion System Structural Integration and Engine Integrity at Monterey, California (September 1974), to appear in AIAA Journal of Aircraft.

12. Robinson, J.N. and Tetelman, A.S., "The Critical Crack-Tip Opening Displacement and Microscopic and Macroscopic Fracture Criteria for Metals," Tech. Report No. 11, UCLA, School of Engineering & Applied Science.

13. Besuner, P.M., "The Application of the Boundary-Integral Equation Method to the Solution of Engineering Stress Analysis and Fracture Mechanics Problems," Report No. FAA-EPRI-75-3-14, March 1975.

14. Key, P.L., "A Relation Between Crack Surface Displacements and the Strain Energy Release Rate," Int. J. Fracture Mechanics, Vol. 5, No. 4, pp. 287-296, Noordhoff Publishing (December 1969).

15. Green, A.E. and Sneddon, I.N., "The Stress Distribution in the Neighborhood of a Flat Elliptical Crack in an Elastic Solid," Proceedings, Cambridge, Phi., Soc., Vol. 46 (1950).

16. Cruse, T.A., "Numerical Evaluation of Elastic Stress Intensity Factors by the Boundary-Integral Equation Method," in The Surface Crack: Physical Problems and Computational Solutions, ed. J. L. Swedlow, ASME 1972.

17. Cruse, T.A., "Application of the Boundary-Integral Equation Method to Three Dimensional Stress Analysis," Journal of Computers and Structures, Vol. 3, 1973, pp. 509-527.

18. Harrison, J.D., "The Analysis of Fatigue Test Results for Butt Welds with Lack of Penetration Defects Using a Fracture Mechanics Approach," pp. 777-789, Second Int. Conf. on Fracture, Brighton, England, 1969.

19. The Surface Crack: Physical Problems and Computational Solutions, ASME Winter Annual Meeting, November 1972.

20. Bueckner, H.F., Weight Functions for the Notched Bar, G.E. Report #69-LS-45, pp. 3-4 (1969).

21. Tetelman, A.S., Besuner, P.M. and Rau, C.A., "Failure Analysis of a Pitman Arm," Failure Analysis Associates, January 1975 (Analytical Results of this Reference Compared Favorably With Unpublished February 1975 Experimental Results by Tetelman, A.S.).

22. Wells, A.A., "The Brittle Fracture Strengths of Welded Steel Plates," Paper No. 6, Meetings of the Institution of Naval Architects, London, 1956.

23. Forman, R.G., et al, "Numerical Analysis of Crack Propagation in Cyclic-Loaded Structures," J. Basic Eng., ASME Trans., Series D, 89, 459 (1967).

24. Yuen, A., Hopkins, S.W., Leverant, G.R., and Rau, C.A., "Correlations between Fracture Surface Appearance and Fracture Mechanics Parameters for Stage II Fatigue Crack Propagation in Ti-6Al-4V," Metallurgical Trans. 5 (August 1974).

25. Gurney, T.R., "An Investigation of the Rate of Propagation of Fatigue Cracks in a Range of Steels," The Welding Institute Members' Report No. E18/12/68.

26. Krishnamurthy, N., "Three-Dimensional Finite Element Analysis of Thick-Walled Vessel-Nozzle Junctions with Curved Transitions, ORNL-TM-3315 (March 1971).

27. Cipolla, R.C., "Computerized Methods to Calculate Stress Intensity Factors Specified in ASME Code, Section XI, Appendix A," April 1975.

28. Rules for Inservice Inspection of Nuclear Power Plant Components, Section XI, ASME Boiler and Pressure Vessel Code, (December 1974).

29. Mager, T.R., et al, "Heavy Section Steel Technology, Report No. 35, p. 46, Westinghouse Electric Corporation Report WCAP-8256, December 1973.

30. Riccardella, P.C. and Mager, T.R., 'Fatigue Crack Growth Analysis of Pressurized Water Reactor Vessels," p. 263, Stress Analysis and Growth of Cracks, Proc., 1971 ASTM Symposium on Fracture Mechanics, 1971.

31. Tracey, D. M., "Three-Dimensional Elastic Singularity Element for Evaluation of K along an Arbitrary Crack Front," Int. J. of Frac. 9, 340-343 (September 1973).

Table I. List of Available Crack-Face Influence Function Solutions to Allow K-Computation for Complex, Arbitrary Stress Distributions

Problem Description(s)	Dimensionality of Elastic Solution	Modes	DOF/M[1]	Error (Maximum Value Quoted by Source)	Published Source(s) (not necessarily comprehensive)	FAA Computer Codes Name[2]/Status[3]			
						K-Calculation	Constant Amplitude Fatigue	Other Capabilities 1	Other Capabilities 2
Center Cracked Plate Under Symmetric Loads (y-Axis symmetry, Fig. 2)	2	I,II,III	1/1	III (exact) I,II (±1%)	(6), Section 3 (See Fig. 2)	IFS2-1/A	IF2-1/A	Residual Mean σ/A	Variable Thickness Approximation
Center Cracked Plate Under Any Loading	2	I,II,III	1/2	III (exact) I,II (±1%)	(6), p. 2.33	--	--	--	--
Single Edge Crack in Finite Strip	2	I,II,III	1/1	III (exact) I,II (±2%)[4]	(6),[4] pp. 227[4]-228, (20)	IFS2-2/B	IF2-1/A	Combined Modes I & II Cycling	Variable Thickness Approx.
Double Edge Crack in Finite Strip	2	I,II,III	1/1	III (exact) I,II (±2%)	(6) p. 2.31	--	--	--	--
Infinite Crack, Infinite Plate	2	I,II,III		exact	(6) p. 3.6	--	--	--	--
Infinite Collinear Cracks, Infinite Plate:									
One Crack Loaded	2	I,II,III	2/2	exact	(6) p. 4.5	--	--	--	--
Two Cracks Loaded Symmetrically	2	I,II,III	1/1	exact	(6) p. 4.6	--	--	--	--
Finite Collinear Cracks in Infinite Plate, Various Loadings of All Cracks	2	I,II,III	1/1 or 1/2	exact	(6) pp. 7.6-7.7	--	--	--	--

Table I (Cont'd)

Program Description(s)	Dimensionality of Elastic Solution	Modes	DOF/M[1]	Error (Maximum Value Quoted by Source)	Published Source(s) (not necessarily comprehensive)	FAA Computer Codes Name[2]/Status[3]			
						K-Calculation	Constant Amplitude Fatigue	Other Capabilities 1	Other Capabilities 2
Infinite Crack Approaching Edge of Half-Space	2	I,II,III	1/1	III (exact) I,II (±1%)	(6) p. 9.5	--	--	--	--
Rows of Infinitely Collinear Infinite Cracks in Infinite Plate	2	III	1/1	exact	(6) p. 13.2	--	--	--	--
Assorted Finite Width and Height Straight Plate Problems	2	--	1,2/ 1,2	Worst Case = ±2%	(6),(8), (1-5)	--	--	--	--
Assorted Finite Width and Height Curved Structure Problems	2	--		Worst Case = ±5%	(8)	--	--	--	--
Infinite Crack in Infinite Solid: Straight Crack Front	3	I,II,III	1/∞	exact	(6) p. 23.1	--	--	--	--
Circular Crack, Arbitrary Mode I Loading, Infinite Solid	3	I	3/∞	exact	(6), p. 24.2	--	--	--	--
Circular Cracks, Internal and External Various Special Cases of Loading, Infinite Solid	2-3	I	1/1	Most are exact	(6), Chap. 25	--	--	--	--
Buried Elliptical Crack Arbitrary Mode I Loading (Infinite Solid)	3	I	4/4	exact	This report, App. C (See Fig.d)	IFS3-1/A	IF3-1/A	--	--

Table I (Cont'd)

Program Description(s)	Dimensionality of Elastic Solution	Modes	DOF/M[1]	Error (Maximum Value Quoted by Source)	Published Source(s) (not necessarily comprehensive)	FAA Computer Codes Name[2]/Status[3]			
						K-Calculation	Constant Amplitude Fatigue	Other Capabilities 1	Other Capabilities 2
Buried Elliptical Crack Arbitrary Mode I Loading (Infinite Solid)	3	I	2/2	exact	(10) (See Fig. 8)	IFS3-2/C	--	--	--
Corner Crack, 1/4 Elliptical Crack, Arbitrary Mode I Loading (Infinite Solid)	3	I	2/2	Three-Dimensional Numerical Stress Analysis	(11) (See Fig. 5)	--	--	--	--
Surface Cracks, 1/2 Elliptical:Corner Crack, 1/4 Elliptical, Arbitrary Mode I, Infinite Mode	3	I	2/2	Combined 3-D and 2-D Eng. Approx.	This report, App. B (See Fig. 7)	IFS3-3/C	IF3-3/C		

[1] M = The number of distinct stress intensity factors that may be computed with the IF solution (e.g., two K values, one for each of two crack tips).

[2] Current FAA computer program and subprogram names.

[3] Status symbols: A = program nearly complete; lacks documentation and user features
B = major portion of program complete but substantial cleanup work is required
C = incomplete program, existing code has been checked out

[4] Refs. (13) and (20) results indicate that Ref. (6) solution is in error.

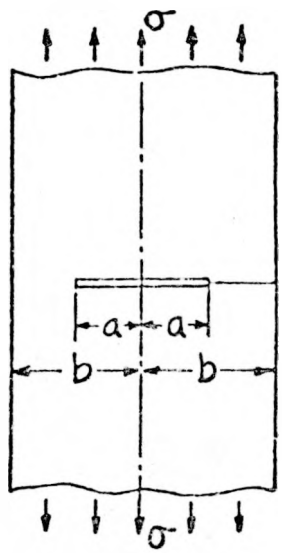

$K(a,b)/\left[\sigma(\pi a)^{1/2}\right]$

a/b	Near Exact Values (0.1% error (6))	IF Calculated Values	Error
0.0005	1.0000	1.0073	0.7%
0.2	1.0246	1.033	0.8%
0.5	1.1867	1.200	1.1%
0.8	1.8160	1.821	0.3%
0.9	2.5776	2.628	2.7%

Table II. Comparison of Published and IF Method-Calculated Stress Intensity Factors for Center-Cracked Plate Under Uniform Stress

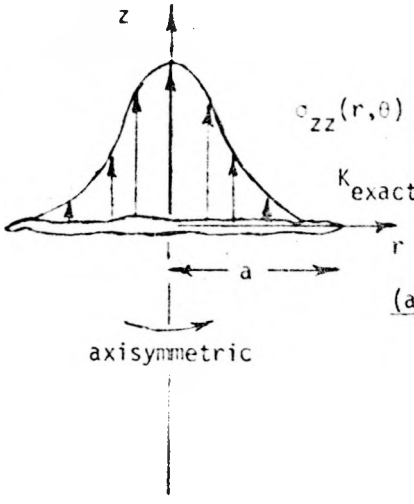

$\sigma_{zz}(r,\theta) = \sigma_{zz}(r) = (1-r^2/a^2)^5$ ksi, $r = (x^2+y^2)^{1/2}$

$K_{exact}(a) = \bar{K}_i(a) = K(a) = \frac{2}{11\pi}(\pi a)^{1/2}$ ksi $\sqrt{in}$, i = x,y

				IF Calculation		
(a in inches)	Exact K(a)	$\bar{K}_i$	Error	$\bar{K}_y$	Error
0.5	0.07253	0.0719	-0.9%	0.0718	-1.1%
1	0.10258	0.1016	-0.9%	0.1015	-1.1%
2	0.14507	0.1438	-0.9%	0.1435	-1.1%
4	0.20516	0.2033	-0.9%	0.2030	-1.1%

Penny-Shaped Crack Cross Section
(Lower Half of Stress Field Not Shown)

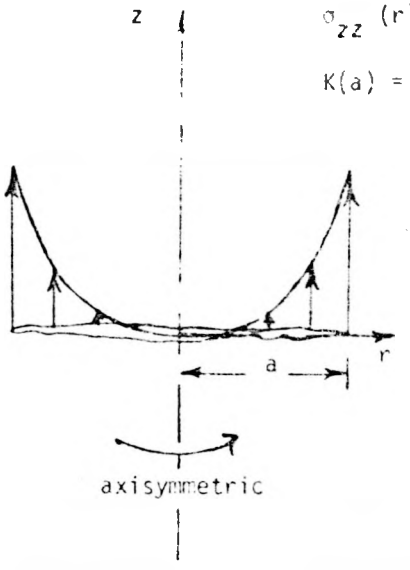

$\sigma_{zz}(r) = r^3$ ksi

$K(a) = \frac{3}{8}(\pi a^7)^{1/2}$ ksi $\sqrt{in}$

(a, r in inches)

				IF Calculation		
a	Exact K(a)	$\bar{K}_x$	Error	$\bar{K}_y$	Error
0.5	0.05875	0.0599	+1.9%	0.0595	+1.3%
1	0.66467	0.6774	+1.9%	0.6730	+1.3%
2	7.51988	7.6639	+1.9%	7.6141	+1.3%
4	85.07777	86.7073	+1.9%	86.1441	+1.3%

Penny-Shaped Crack Cross Section
(Lower Half of Stress Field Not Shown)

Table III. Comparison of Exact (6) and IF Method-Calculated Stress Intensity Factors for Penny-Shaped Crack in Infinite Solid Under Two Complex Symmetric Stress Fields.

Table IV. Summary of Six Fatigue Analyses of the Weld Crack in Figure 9

Case #	Width of Structure (in.)	Alternating Stress, $\Delta\sigma$ (ksi)	Mean Stress Components (ksi)		Fig. # for Fatigue Anal. Results	Calculated Cycles From 2a=0.25" to Failure
			Uniform	Residual		
1	2000	25	12.5	See App. D	11	18009
2	2000	25	-17.5	App. D	11	∞
3	10	25	12.5	Fig. 9 + App. D	10	17949
4	10	25	-17.5	Fig. 9	10	∞
5	2000	25	12.5	0	11	107439
6	10	25	12.5	0	10	95852

Table V. Cumulative Damage Analysis of Nozzle Alternating Stresses Caused by Eleven Distinct Types of Load Transients

i	ith Load Transient	Peak $\Delta\sigma_i$ (ksi)	Expected Number of Transients in 40 Year Life = n_i	Damage Measure $y_i = 10^{-8}\, n_i\, \Delta\sigma_i^{3.726}$	Equivalent # of Heatup-Cooldown (i=1) Transients in 40 Years $e_i = n_1 y_i / y_1$
1	Heatup-Cooldown	31.7	200	0.7834	200
2	Plant Loading and Unloading	7.4	18400	0.3188	81.4
3	Power Step Change	4.2	2000	0.0042	1.1
4	Steam Drop	11.5	200	0.0179	4.6
5	Steady State Fluctuations	0.2	1,000,000	0.0000	0
6	Loss of Load	0.9	80	0.0000	0
7	Loss of Flow	22.6	80	0.0888	22.7
8	Reactor Trip	7.3	400	0.0066	1.7
9	Turbine Roll Test	11.0	10	0.0008	0.2
10	Cold Hydro Test	45.7	5	0.0765	19.5
11	Hot Hydro Test	31.2	40	0.1477	37.7
Σ				1.4447	368.9

For each Heatup-Cooldown cycle, the upper bound crack growth rate is (28): $\frac{da}{dN_1}$ (in/cyc) = $.3795 \times 10^{-9}\, \Delta K_{II}^{3.726}$

so that for the 40-year lifetime increments $N_{40} = 368.9\, N_1$: $\frac{da}{dN_{40}} = 368.9\,(.3795 \times 10^{-9})\, \Delta K_{II}^{3.726} = 1.4 \times 10^{-7}\, \Delta K_{II}^{3.726}$

as in Equation (6.1) of the text.

TABLE VI

COMPARISON OF $\dot{k}$ AND $\bar{K}$ FOR SEVERAL CASES OR SURFACE AND CORNER CRACKS UNDER UNIFORM NORMAL PRESSURE σ_o VALUES GIVEN ARE $K = \frac{K}{2\sigma_o\sqrt{a/\pi}}$

GEOMETRY	r	$\bar{K}_x$	K_x	$\bar{K}_y$	$\dot{K}_y$
Embedded Ellipse	1	1.00	1.00	1.00	1.00
	∞	1.46	1.57	1.03	0.0
Surface Half-Ellipse	1	1.11	1.04*	1.16	1.26*
	∞	1.65	1.77	1.17	?
Corner Quarter-Ellipse	1	1.26	1.28*	1.26	1.28*
	∞	1.89	?	1.22	?

*Taken from Tracey (31)

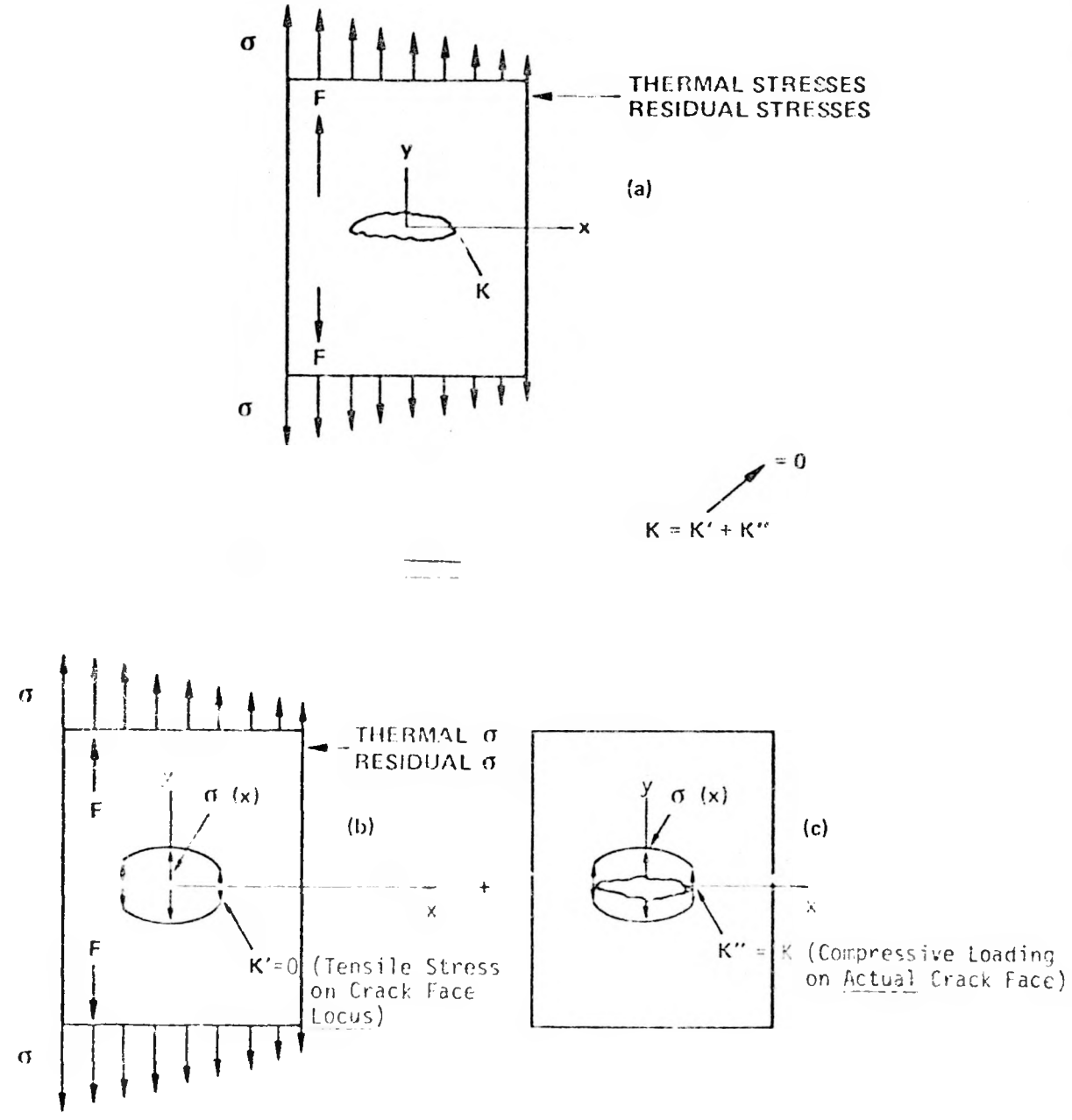

Fig. 1. The Reduction of a Problem, (a), Into Two Simpler Problems, (b) and (c), for Computations of Stress Intensity Factor (from Reference 3, illustrated for a Center-Cracked Infinite Plate)

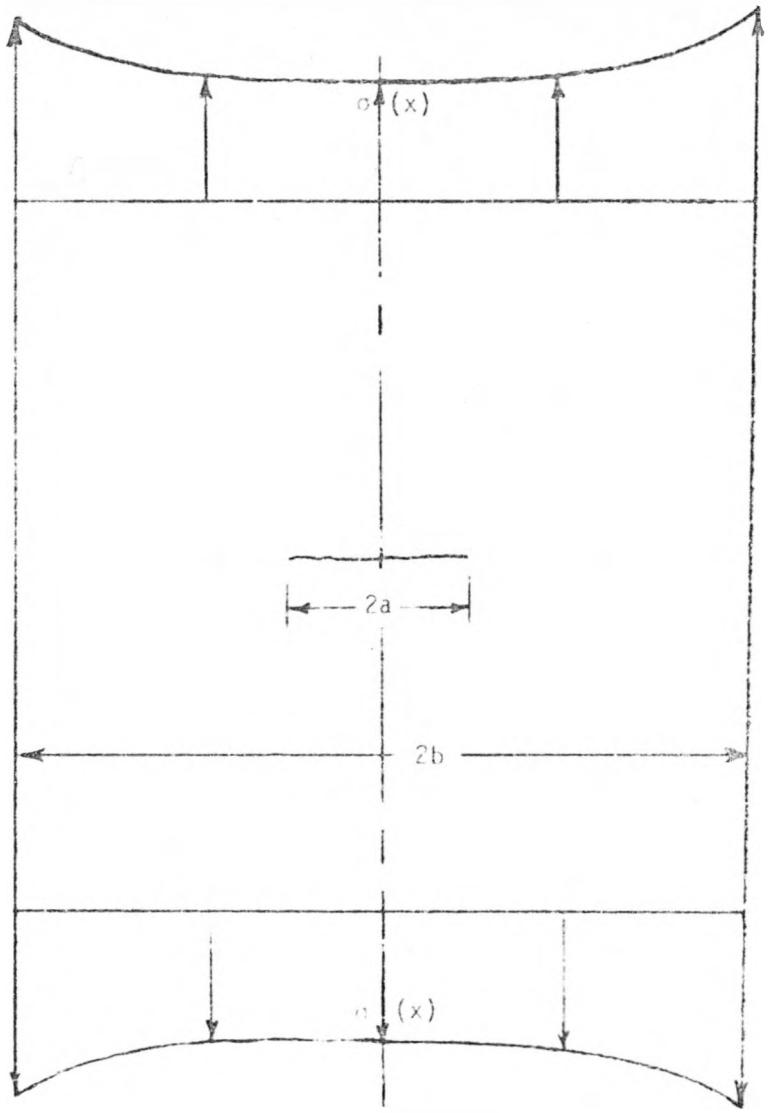

Fig. 2. Center-Cracked Plate Under Symmetric Stress

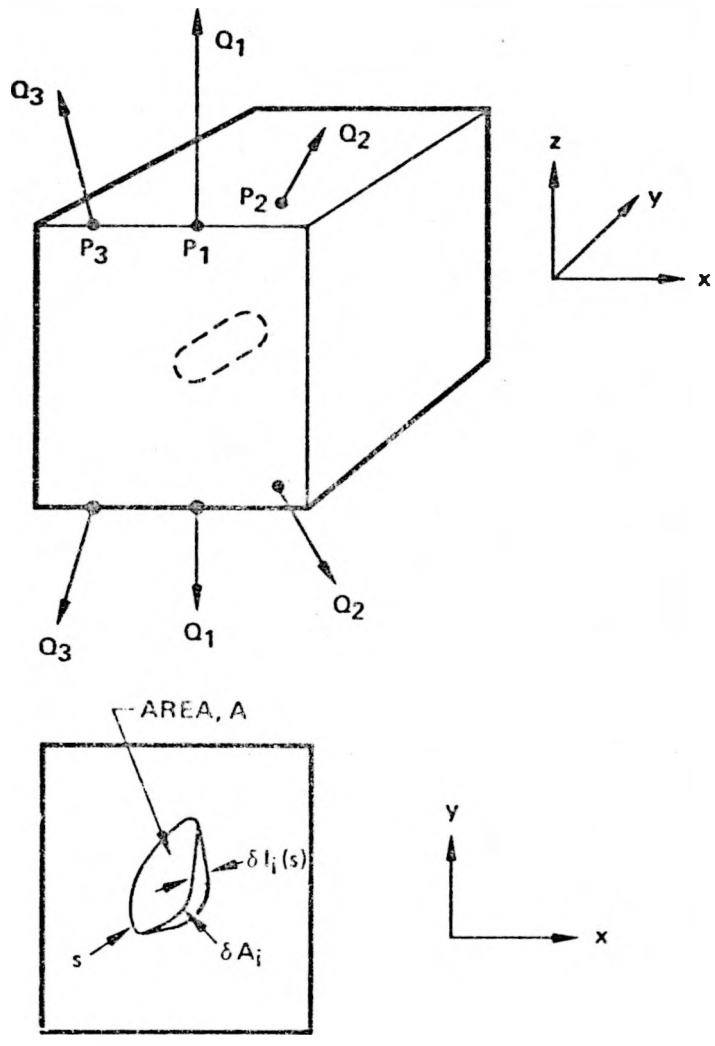

Fig. 3. Schematic of Prescribed Normal Perturbation $\{\delta l_i(s)\}$ of Crack Front

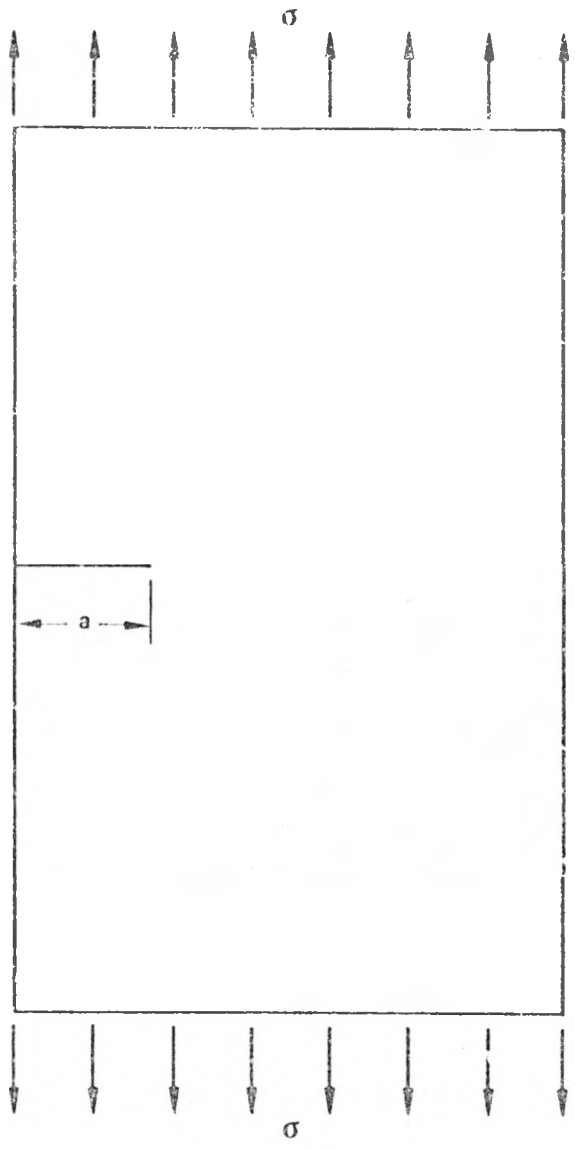

Fig. 4a. Through-The-Thickness Edge Crack in a Finite Width Plate

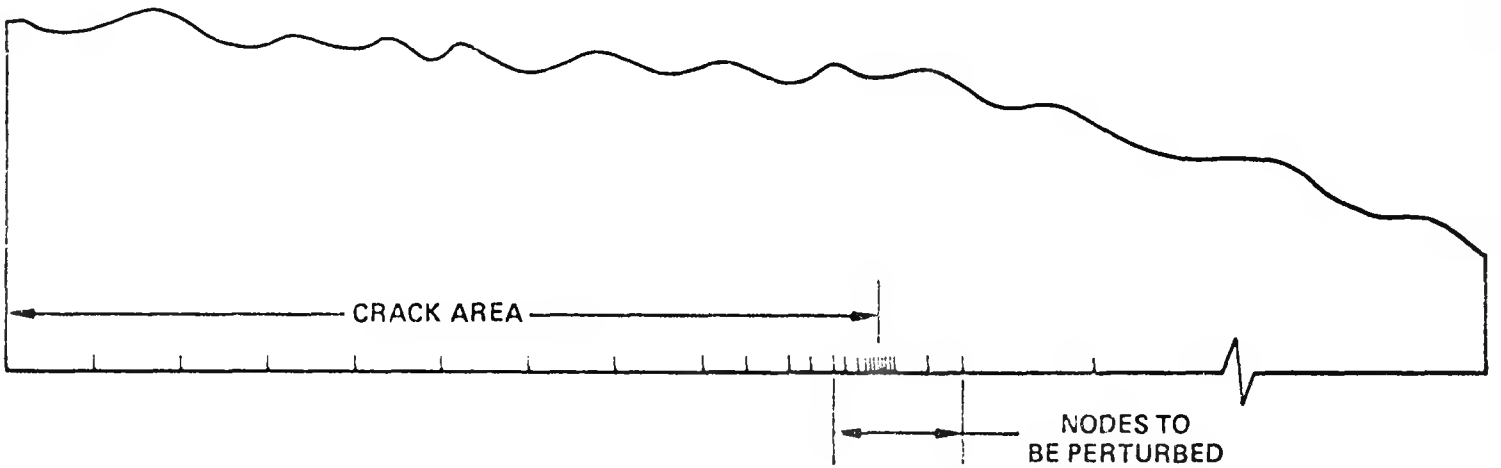

Fig. 4b. 2-D Bie Crack Surface Break-Up

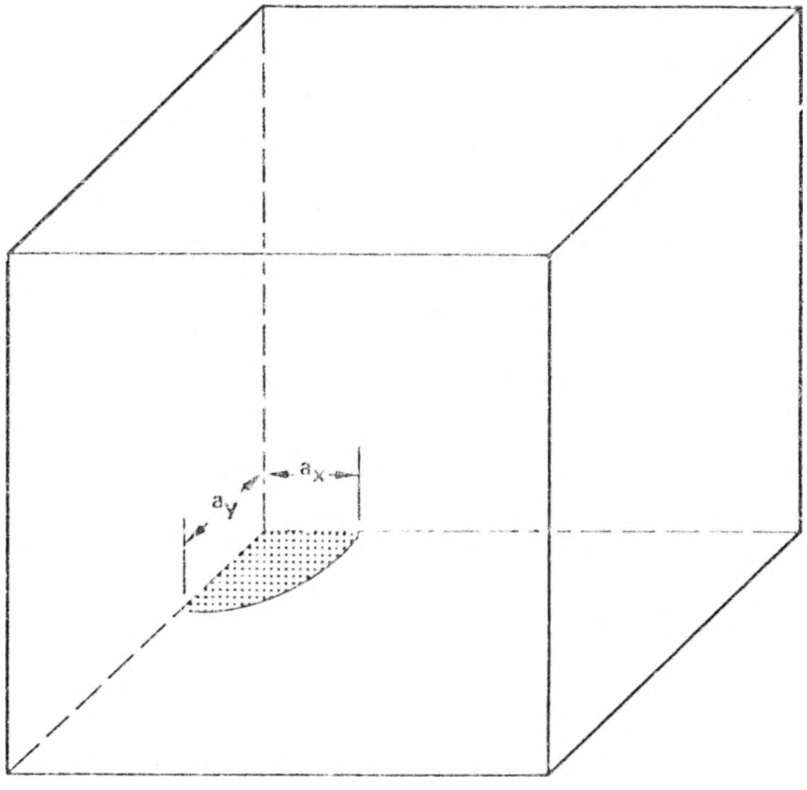

Fig. 5a. Symmetric Three-Dimensional Boundary-Integral Equation Model of a Corner Crack in an Infinite Body

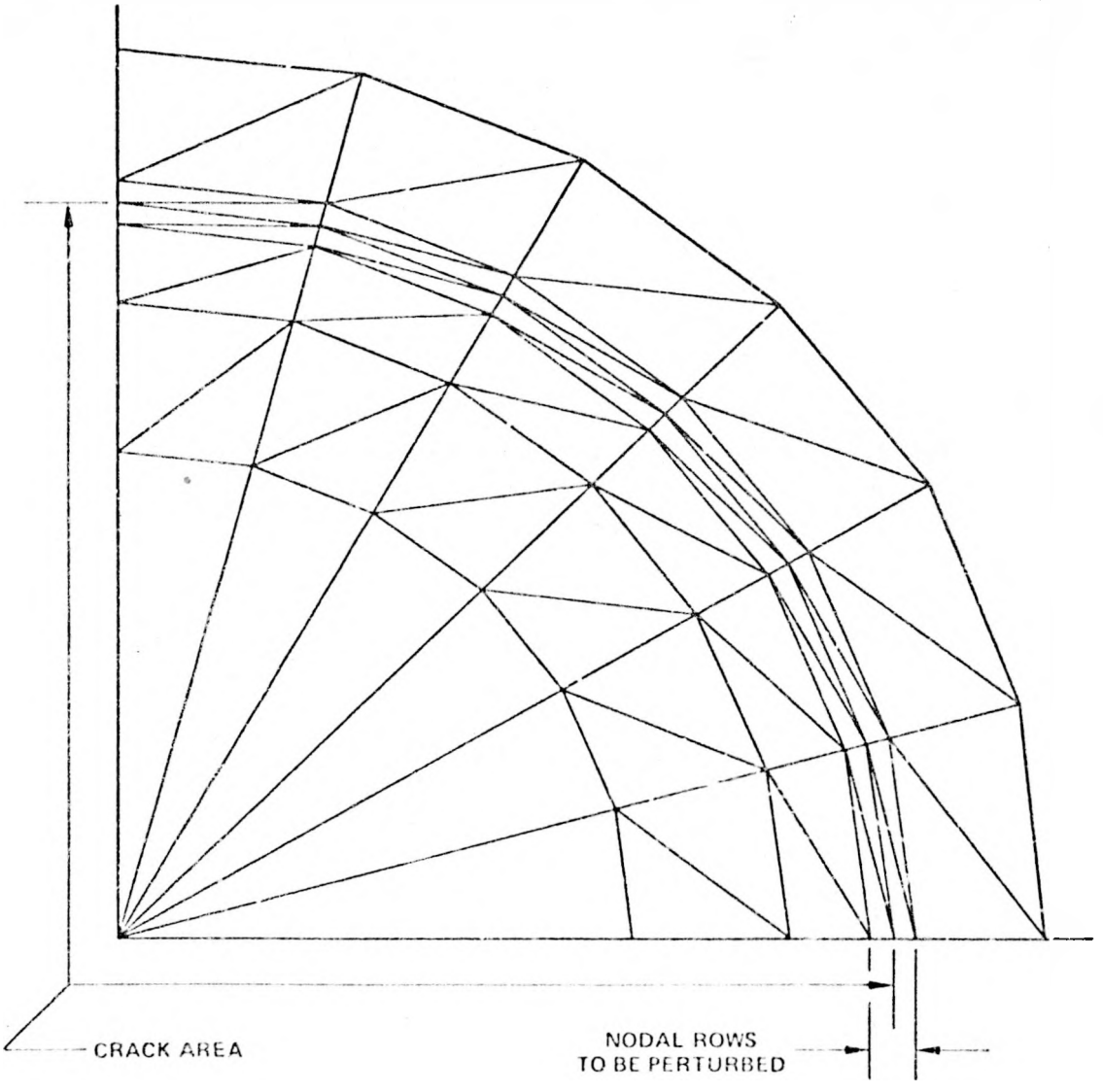

Fig. 5b. 3-D Bie Crack Surface Break-Up

FREEDOM a_x :

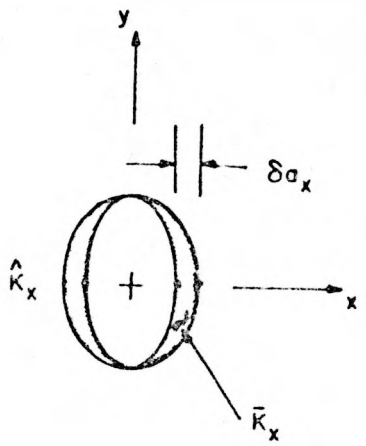

$$\bar{K}_x^2 = \frac{1}{\delta A_x} \iint_{\delta A_x} K^2(s)\, dA$$

$$\hat{K}_x = K(\pm a_x, 0)$$

$$\delta A_x = \pi\, a_y\, \delta a_x$$

FREEDOM a_y :

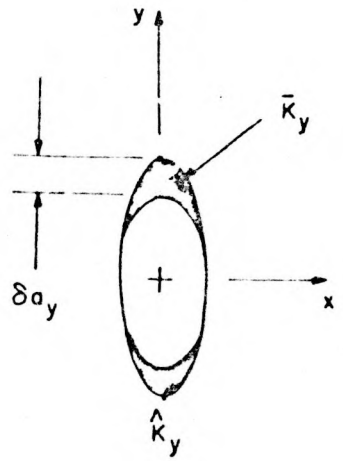

$$\bar{K}_y^2 = \frac{1}{\delta A_y} \iint_{\delta A_y} K^2(s)\, dA$$

$$\hat{K}_y = K(0, \pm a_y)$$

$$\delta A_y = \pi\, a_x\, \delta a_y$$

Fig. 6. A Two DOF Buried Elliptical Crack

HALF-ELLIPSE SURFACE CRACK

INFLUENCE FUNCTION CORRECTION FACTOR
$f_s(x_s)$

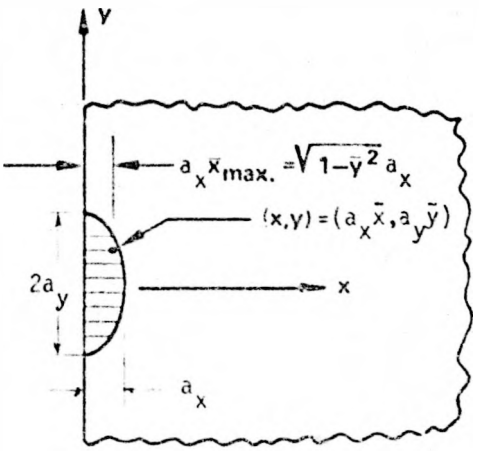

QUARTER ELLIPSE CORNER CRACK

INFLUENCE FUNCTION CORRECTION FACTOR
$f_s(x_s) + f_s(y_s) - 1$

WHERE $x_s = \frac{\bar{x}}{\bar{x}_{max.}}$, $y_s = \frac{\bar{y}}{\bar{y}_{max.}}$

f_s = 2-D CORRECTION FACTOR FOR SURFACE CRACK

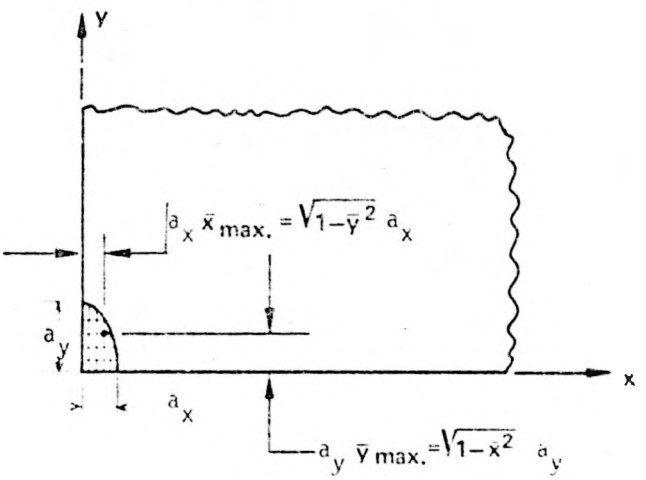

Fig. 7. Approximate Near-Surface Correction Factors for 3-D Surface and Corner Crack Influence Functions

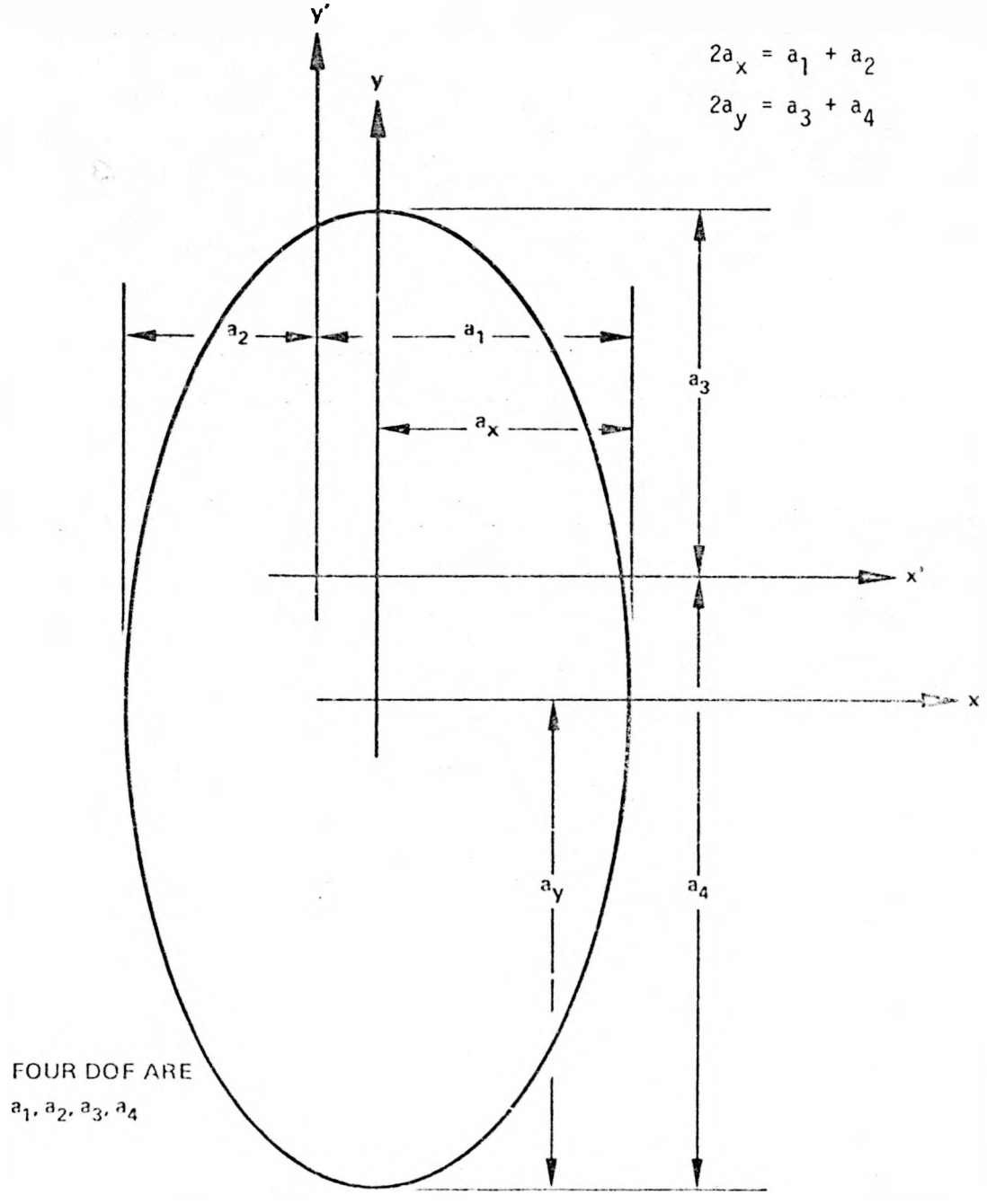

Fig. 8. Dimensions of a 4 DOF Buried Elliptical Crack

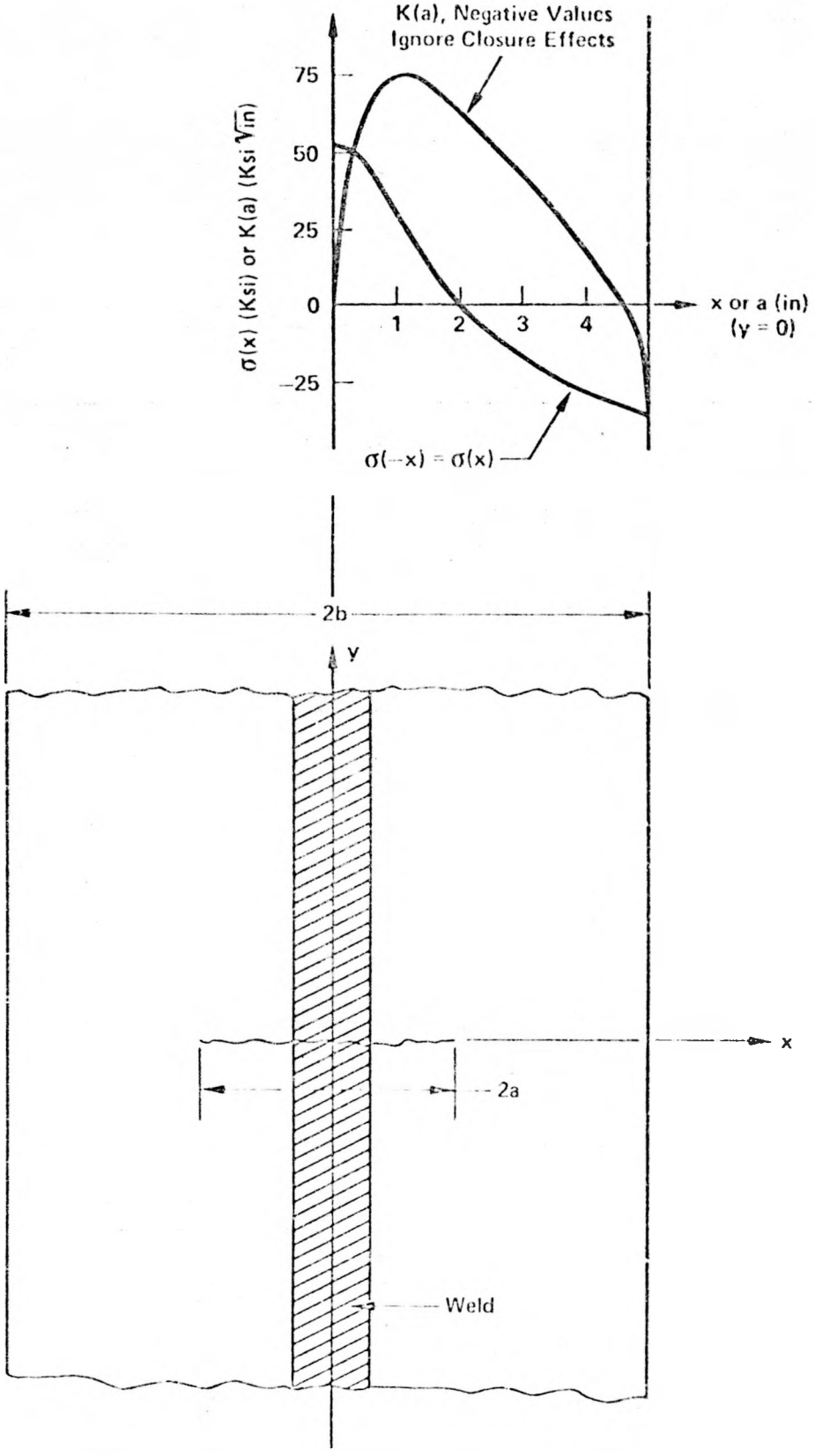

Fig. 9. Weld-Induced Symmetric Residual Stress, $\sigma(x)$, in an Uncracked Specimen and Resulting Stress Intensity Factor K(a) When a Center-Crack of Length, 2a is Introduced

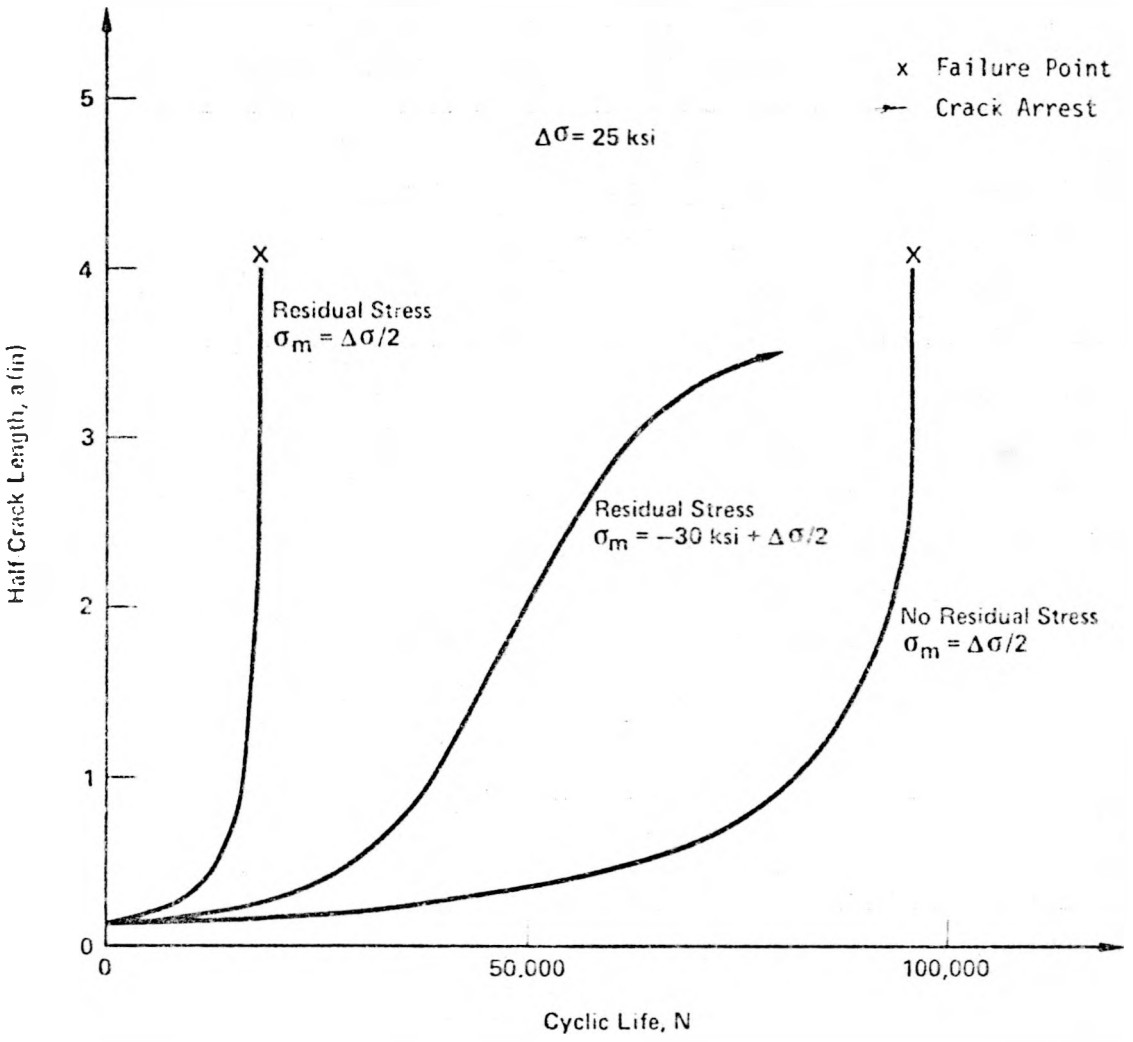

Fig. 10. Weld Crack Propagation in a 10-Wide Specimen for Three Mean Stress Distributions

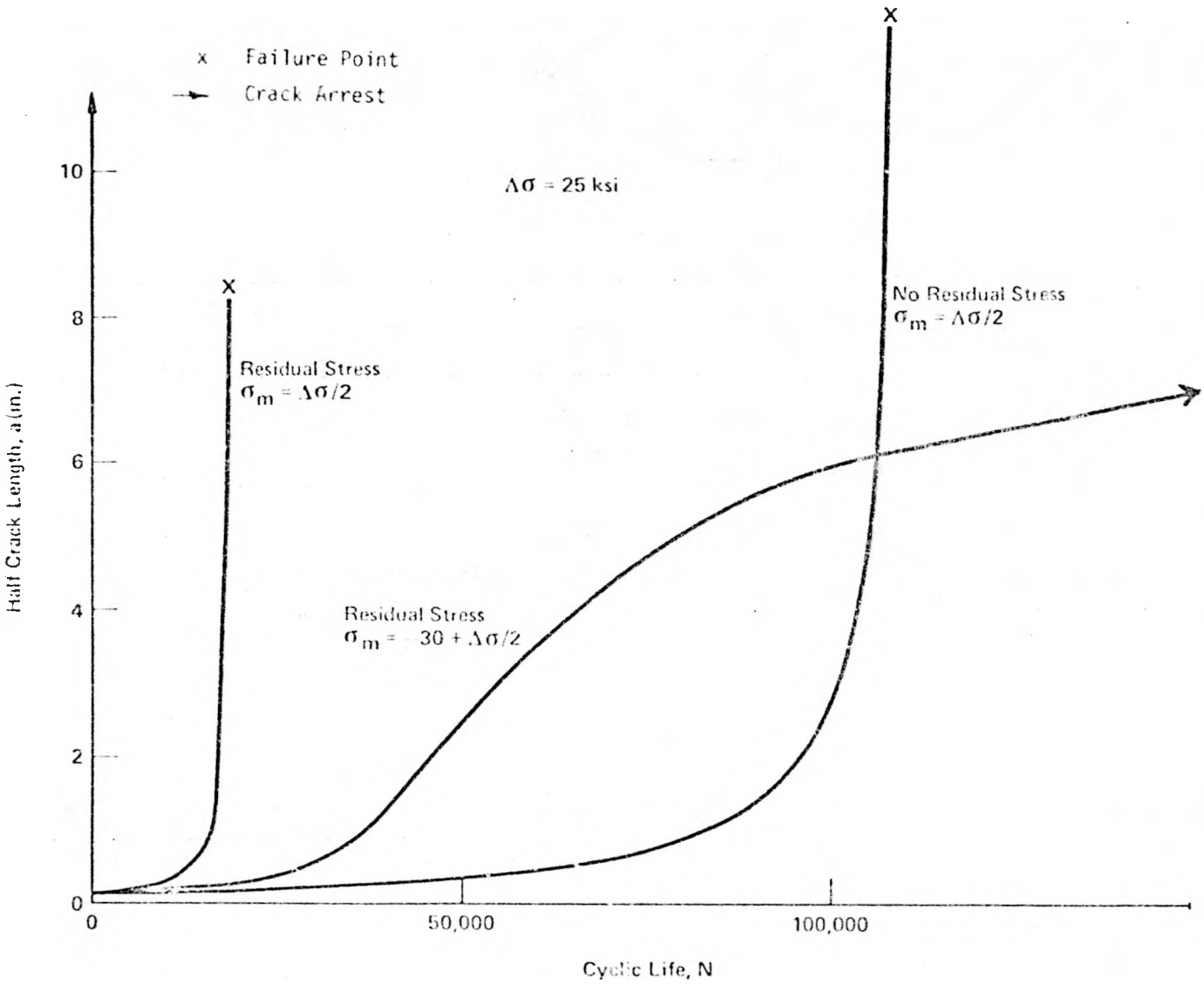

Figure 11. Weld Crack Propagation in a Large Pipe for Three Mean Stress Distributions

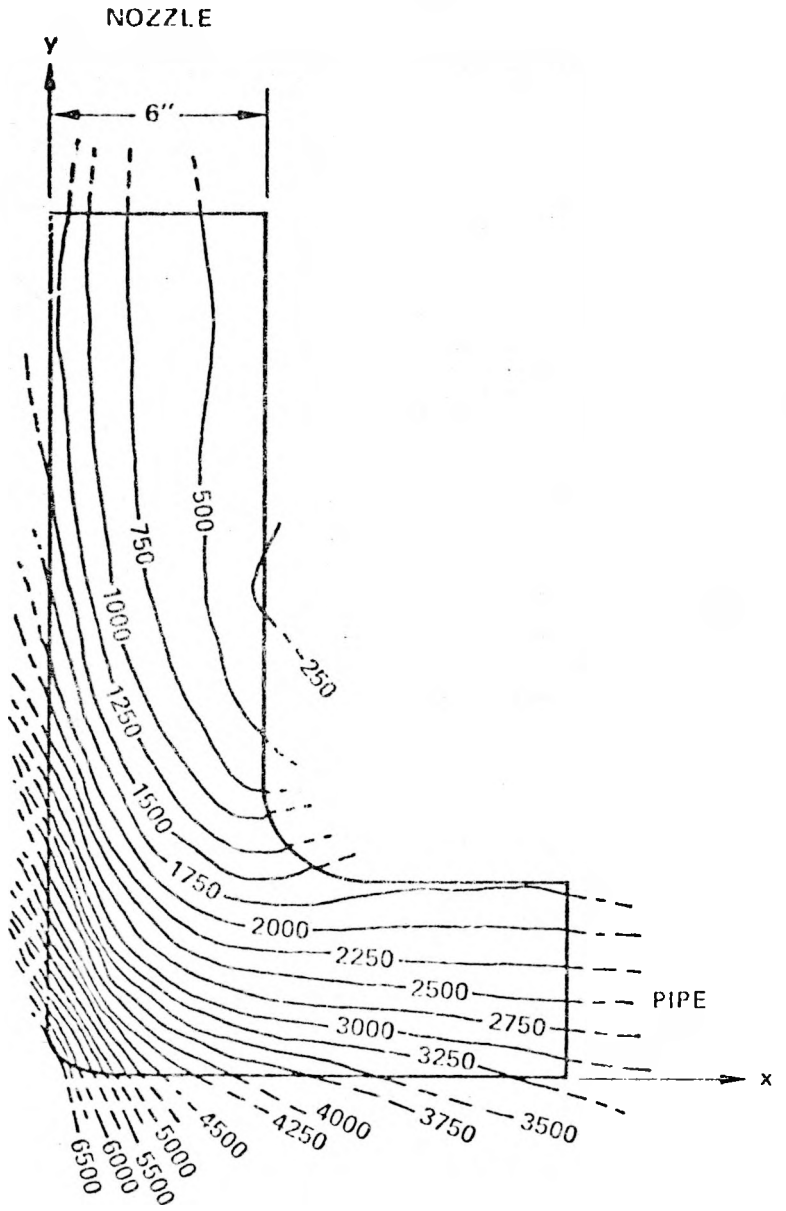

Fig. 12. Circumferential Stress Contours, $\sigma_{zz}(x,y)$ (psi) for 1000 psi Internal Pressure

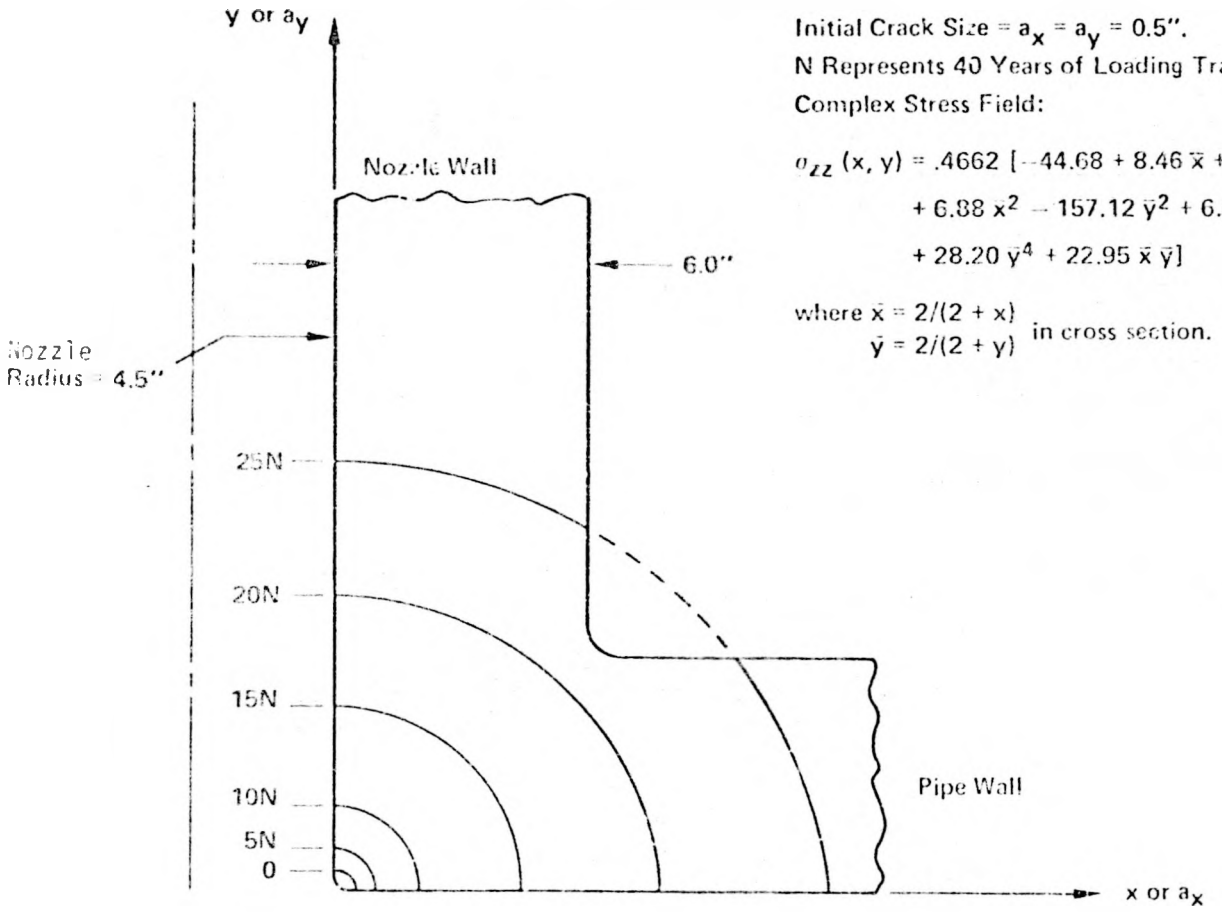

Fig. 13
Growth of Elliptical Corner Crack
at a Symmetric Cross Section of an HSST
Program, Intermediate Test Vessel, Pipe Nozzle Junction